

Contract No:

This document was prepared in conjunction with work accomplished under Contract No. DE-AC09-08SR22470 with the U.S. Department of Energy (DOE) Office of Environmental Management (EM).

Disclaimer:

This work was prepared under an agreement with and funded by the U.S. Government. Neither the U. S. Government or its employees, nor any of its contractors, subcontractors or their employees, makes any express or implied:

- 1) warranty or assumes any legal liability for the accuracy, completeness, or for the use or results of such use of any information, product, or process disclosed; or
- 2) representation that such use or results of such use would not infringe privately owned rights; or
- 3) endorsement or recommendation of any specifically identified commercial product, process, or service.

Any views and opinions of authors expressed in this work do not necessarily state or reflect those of the United States Government, or its contractors, or subcontractors.



Savannah River
National Laboratory®

A U.S. DEPARTMENT OF ENERGY NATIONAL LABORATORY • SAVANNAH RIVER SITE • AIKEN, SC

An Assessment of the Materials of Construction for the Transfer Lines and Unit Operations Equipment Associated with the Recycle Diversion Process

B. J. Wiersma

June 2021

SRNL-STI-2021-00252, Revision 0

SRNL.DOE.GOV

DISCLAIMER

This work was prepared under an agreement with and funded by the U.S. Government. Neither the U.S. Government or its employees, nor any of its contractors, subcontractors or their employees, makes any express or implied:

1. warranty or assumes any legal liability for the accuracy, completeness, or for the use or results of such use of any information, product, or process disclosed; or
2. representation that such use or results of such use would not infringe privately owned rights; or
3. endorsement or recommendation of any specifically identified commercial product, process, or service.

Any views and opinions of authors expressed in this work do not necessarily state or reflect those of the United States Government, or its contractors, or subcontractors.

Printed in the United States of America

**Prepared for
U.S. Department of Energy**

Keywords: *Corrosion, Erosion-corrosion,
Wiped Film Evaporator, DWPF Recycle*

Retention: *Permanent*

An Assessment of the Materials of Construction for the Transfer Lines and Unit Operations Equipment Associated with the Recycle Diversion Process

B. J. Wiersma

June 2021

Prepared for the U.S. Department of Energy under
contract number DE-89303320REM000063.



REVIEWS AND APPROVALS

AUTHORS:

B. J. Wiersma, Materials Technology Directorate
Environmental and Legacy Management Division

Date

TECHNICAL REVIEW:

M. R. Duignan, Reviewed per E7 2.60
Chemical Processing Directorate
Environmental and Legacy Management Division

Date

APPROVAL:

J. Manna, Director
Materials Technology Directorate
Environmental and Legacy Management Division

Date

F. M. Pennebaker, Director
Chemical Processing Directorate
Environmental and Legacy Management Division

Date

D. T. Wallace, Manager
Project Engineering Manager
DWPF Recycle Diversion

Date

ACKNOWLEDGEMENTS

I would like to thank Mark Duignan, Chris Martino, Frank Pennebaker and Joseph Manna of the Savannah River National Laboratory for their careful technical review of this document. I would also like to acknowledge William King for providing input on the anticipated chemistry of the recycle diversion stream. I would also like to thank William Holtzscheiter, Arthur Wiggins, Stephanie Harrington, Rachel Seeley, Noel Chapman, and Christine Baker of Savannah River Remediation for their technical review and comments on the document. Finally, I would like recognize Shawn Campbell, Cameron Joslyn, and Dale Halgren, all of Washington River Protection Solutions. They provided information on the performance of the Thin Film Dryer that is in use at the Hanford Effluent Treatment Facility. Finally, this report was composed during the COVID-19 pandemic and was for the most part written at home while teleworking. I would like to thank my wife and family for providing an atmosphere where I could focus and complete the report.

EXECUTIVE SUMMARY

The Defense Waste Processing Facility (DWPF) processes and vitrifies radioactive waste that it receives from the Concentration, Storage, and Transfer Facility (CSTF) and Salt Waste Processing Facility (SWPF). As a result of the evaporation of water during both the melter feed preparation and the melter feed vitrification steps in DWPF, a recycle waste stream is generated, neutralized, and sent back to the CSTF. The recycle waste is a dilute water stream originating from the collection of condensate liquids containing some minor sludge and frit solids and other waste components primarily resulting from entrainment into the condensate during foam-over events. The recycle stream volume is significant and is expected to approach 3 million gallons per year once the SWPF reaches full operation. Diverting the bulk of the recycle waste stream from the CSTF is essential for the eventual closure of the waste tanks, and hence the completion of the SRS liquid waste mission.

Cross flow filtration (CFF) and wiped film evaporation (WFE) were selected as the preferred technologies for processing the recycle stream. This evaluation assessed the influence of pH (i.e., expected feed range from 9-13) on the potential for corrosion and erosion-corrosion in the transfer lines, the CFF and the WFE. The baseline chemistry being developed for the recycle diversion (RD) process was utilized to evaluate the influence of pH. The possibility that the undissolved solids in the feed may result in erosion in the WFE was also assessed. Other mechanical failure modes such as fatigue were also evaluated.

This evaluation reviewed the literature on the performance of stainless steel and nickel-based alloys at the proposed RD process chemistry, identified potential gaps in the data, and recommended testing. The conclusions and recommendations for the transfer lines and unit operations are presented below.

Transfer Lines

- The RD process chemistry conditions are similar to those that were evaluated previously. The previous evaluation concluded that no accelerated corrosion or erosion-corrosion of the 304L pipelines would be anticipated. Recent testing for the glycolic flowsheet and the glycolate destruction process indicated a low susceptibility to corrosion at the current conditions as well.
- However, the testing conditions were at pH 13, whereas a minimum pH of 9 is proposed for the RD process. Screening tests to confirm that accelerated general, localized corrosion, and erosion-corrosion do not occur at the lower bound pH are recommended.

Cross Flow Filters

- The RD process chemistry and the filter cleaning operation were reviewed and compared to data in the literature. Literature data from corrosion testing performed on sintered

316L stainless steel materials indicates that they have a low propensity for general or localized corrosion.

- No tests were performed to assess the CFF for susceptibility to erosion-corrosion under the Hanford Low Activity Waste Pretreatment System (LAWPS) test conditions. As with the transfer lines, a screening test (e.g., rotating cylindrical electrode) is recommended to confirm that the sintered 316L stainless steel is not susceptible to erosion-corrosion. These tests should cover a range of pHs that considers the filter cleaning process as well as the pH of the RD process stream.

Wiped Film Evaporators

- The performance of materials during pilot-scale and full-scale demonstrations, as well as field performance was reviewed.
- The failure analysis of the WFE for the Hanford Effluent Treatment Facility indicated that the 316L stainless steel blades had failed by chloride stress corrosion cracking, corrosion fatigue or fatigue.
- Some of the failures of WFEs in pilot-plant studies and actual service have been external to the vessel, where the blades and heat transfer system are located. The failure mechanisms have been fatigue or wear (erosion) of bearings and seals due to the movement and/or misalignment of the rotating shaft. These failures in some instances have resulted in erosion of the agitator blades and light scarring of the heat transfer surface. Careful design of the shaft train (i.e., consideration of both thermal and mechanical stresses), material selection (e.g., avoid situations where tungsten-carbide contacts the waste), and plans for maintenance of these areas that avoid contamination and dose exposure are recommended. Due to the moving shaft, failure mechanisms such as erosion or fatigue may happen. The risk, probability, and consequence of failure may be minimized by designing the WFE with these considerations in mind.
- The temperature of the WFE for the RD process is anticipated to be either 60 °C or the atmospheric boiling point of the waste (~120 °C). From a corrosion standpoint, if the temperature is 60 °C or less for the RD process chemistry, data indicate that a 300 series stainless steel would likely be appropriate for the vessel and the heat transfer surface. On the other hand, for temperatures approaching 120 °C, a nickel-based alloy such as G30 or Ultimet, which is used for the bent tube evaporator (BTE) tube bundle, may be more suitable for long term service.
- There have been no long-term erosion-corrosion studies for either the 300 series stainless steel or the nickel-based alloy conducted at the RD process conditions. As with the transfer lines and the CFF, a screening test (e.g., rotating cylindrical electrode) is recommended to confirm that the stainless steel and the nickel-based alloys are not susceptible to erosion-corrosion. The results of these tests could be used to determine conditions for longer term tests, if needed (e.g., slurry pot). Engineering models may also be used to assess the likelihood of erosion of the blade and heat transfer surface

given the wt.% of undissolved solids and the slurry abrasive velocity generated by the movement of the WFE blades.

TABLE OF CONTENTS

LIST OF TABLES	xi
LIST OF FIGURES.....	xii
LIST OF ABBREVIATIONS.....	xiii
1.0 Introduction.....	1
2.0 Degradation Mechanisms.....	3
2.1 Corrosion.....	4
2.2 Erosion	6
2.3 Erosion-Corrosion.....	7
2.4 Fatigue.....	8
3.0 Literature Review of Transfer Line and Unit Operations in RD Environments.....	9
3.1 Transfer Lines.....	9
3.1.1 Summary of Corrosion and Erosion-corrosion testing for SRS	9
3.1.2 Corrosion Testing in Support of Glycolic Acid Flowsheet.....	14
3.1.3 Erosion-Corrosion.....	16
3.1.4 Thermal Fatigue.....	18
3.2 Cross Flow Filters.....	19
3.2.1 SRNL Corrosion Testing for LAWPS Cross Flow Filter Materials.....	19
3.2.2 Flow-through Tests for Hanford LAWPS Cross Flow Filters.....	20
3.3 Wiped Film Evaporator Corrosion and Erosion-Corrosion Testing.....	23
3.3.1 SRL Testing (1975-1982).....	23
3.3.2 SRL Testing for the Uranium Solidification Facility (1988-1989).....	26
3.3.3 WFE Tests at Oak Ridge National Laboratory Supporting Disposition of Melton Valley Waste	28
3.3.4 Low Temperature, Vacuum WFE Developed by Columbia Energy	31
3.3.5 Thin Film Dryer for Hanford Effluent Treatment Facility.....	35
3.3.6 Agitator Blade Performance in DWPF Sludge/Frit Slurries	40
3.4 Bent Tube Evaporator Degradation and Failures.....	42
3.4.1 Corrosion Testing for Evaporator Materials.....	42
3.4.2 Failure Analysis of the 242-25H Evaporator Shell.....	45
4.0 Anticipated Chemistry and Temperature Process Variables for the Recycle Diversion Process.....	47
5.0 Assessment of Gaps and Recommendations for Testing	49
5.1 Transfer Lines.....	49
5.2 Cross Flow Filters.....	50

5.3 Wiped Film Evaporators..... 50

6.0 Conclusions..... 51

7.0 References..... 52

LIST OF TABLES

Table 2-1 Chemical and Mechanical Degradation Mechanisms.....	3
Table 2-2 Environmental and Material Factors that Influence Corrosion	4
Table 3-1. Molar Anion Concentrations for Simulated Waste Solutions Tested at SRNL.....	10
Table 3-2. General Corrosion Rates for 304L Stainless Steel Exposed to Simulated Waste Environments at SRNL. Rates are in mils per year (mpy).....	10
Table 3-3. Molar Anion Concentrations for Simulated Waste Solutions Tested at PNL.	11
Table 3-4. General Corrosion Rates for 304L Stainless Steel Exposed to Simulated Waste Environments at PNL. Rates are in mils per year (mpy).....	11
Table 3-5 Simulant Compositions for Glycolic Acid Flowsheet Testing for 304L.....	15
Table 3-6. Recycle Collection Tank (RCT) Simulant Composition.....	16
Table 3-7. Molar Anion Concentrations for Simulated Waste Solutions Tested at PNL.	18
Table 3-8. Chemical Analysis for Master Batch of PEP Supernate.	20
Table 3-9. Solution Compositions for 304L Exposure Tests.....	27
Table 3-10. Corrosion Rates for 304L Stainless Steel in Acidic Uranyl Nitrate Solutions.	28
Table 3-11. Liquid Waste Simulants for Pilot-Scale WFE Testing at ORNL.....	30
Table 3-12. Sludge Solids for Simulants for Pilot-Scale WFE Testing at ORNL.....	30
Table 3-13. Process Parameter Values for WFE Testing at ORNL.	30
Table 3-14. Waste Simulant Compositions for WFE Pilot Scale Tests.....	33
Table 3-15 Groundwater Chemistry for TFD (70% operation).....	36
Table 3-16 Process Condensate Chemistry for TFD (30% Operation).	37
Table 3-17. Composition of Simulated Alkaline Evaporator Solution.....	43
Table 3-18. Composition of Simulated Acidic Evaporator Solution	44
Table 4-1. SMECT and OGCT Compositions (RCT Feed).....	48
Table 4-2. Estimated RCT and Recycle Diversion Evaporator Pot Major Species Concentrations Assuming 20.3x Evaporator Concentration Factor, and No Manganese Precipitation.....	49

LIST OF FIGURES

Figure 2-1 Potential vs. Current Diagram Illustrating Corrosion Behavior.....	4
Figure 2-2 Spectrum of Corrosion and Erosion-Corrosion Behavior.....	7
Figure 3-1. Section of core pipe from clean-out-port #3: (a) Dye penetrant test showing cracks on the interior of the pipe, (b) Micrograph showing transgranular chloride SCC.....	13
Figure 3-2. Sintered 316L material at 1000X magnification.	19
Figure 3-3. Set-up for CFF flow through tests.	22
Figure 3-4. Post-test CFF filter media samples after cleaning.	22
Figure 3-5. Schematic of Horizontal WFE.	23
Figure 3-6. Schematic of Vertical WFE.	24
Figure 3-7 Large fatigue striations with finer secondary striations perpendicular to the primary striations.	25
Figure 3-8. Optical micrograph of sensitized 304L stainless steel microstructure (500 X magnification).	26
Figure 3-9. SEM image of surface of specimen after vapor phase exposure, showing IGA (500X magnification).	27
Figure 3-10. SEM image of cross-sectioned specimen showing IGA depth of attack in the liquid exposed metal. The dashed line indicates the level of the original surface and the arrow points to the deepest IGA penetration (250x magnification).	28
Figure 3-11. WFE for Pilot-Scale Tests at ORNL.....	29
Figure 3-12. CEES Pilot Scale WFE System.....	32
Figure 3-13. Pilot Scale Rotatherm WFE.	32
Figure 3-14. Full-Scale Rotatherm WFE.	34
Figure 3-15. Hanford ETF Thin Film Dryer.	35
Figure 3-16 Schematic of an LCI TFD taken from Product Literature 2021.....	36
Figure 3-17 Macroscopic view of failed blade tip.....	38
Figure 3-18. Failure by Chloride SCC or Corrosion Fatigue (see upper left).....	38
Figure 3-19 Failure by Fatigue.....	39
Figure 3-20. Failed TFD rotor hinge.	40
Figure 3-21. Erosion Test Apparatus Results.....	41
Figure 3-22. Leakage from 3H Evaporator Shell.	46

Figure 3-23. Leakage from the Bottom Spherical Head of the 3H Evaporator..... 46

LIST OF ABBREVIATIONS

BTE	Bent Tube Evaporator
CEES	Columbia Energy and Environmental Services
CFF	Cross Flow Filter
CPP	Cyclic Potentiodynamic Polarization
CSTF	Concentration, Storage and Transfer Facility
CTS	Concentrate Transfer System
DST	Double Shell Tank
DWPF	Defense Waste Processing Facility
EPDM	Ethylene Propylene Diene Monomer
ETA	Erosion Test Apparatus
ETF	Effluent Treatment Facility
FAC	Flow Assisted Corrosion
IGA	Intergranular Attack
LAW	Low Activity Waste
LAWPS	Low Activity Waste Pretreatment System
LLLW	Low Level Liquid Waste
LPPP-RPT	Low Point Pump Pit – Recycle Pump Tank
MIC	Microbiologically Influence Corrosion
MOC	Materials of Construction
mpy	mils per year
NAS	Sodium Aluminosilicate
OGCT	Off-gas Condensate Tank
ORNL	Oak Ridge National Laboratory
PEP	Pretreatment Engineering Platform
PNL	Pacific Northwest Laboratory
RCT	Recycle Collection Tank
RD	Recycle Diversion
SCC	Stress Corrosion Cracking
SEE	Systems Engineering Evaluation
SEM	Scanning Electron Microscope
SME	Slurry Mix Evaporator

LIST OF ABBREVIATIONS (cont.)

SMECT	Slurry Mix Evaporator Condensate Tank
SRAT	Slurry Receipt Adjustment Tank
SRL	Savannah River Laboratory
SRNL	Savannah River National Laboratory
SRR	Savannah River Remediation
SRS	Savannah River Site
SRTC	Savannah River Technology Center
SST	Single Shell Tank
SWPF	Salt Waste Processing Facility
TFD	Thin Film Dryer
TIC	Total Inorganic Carbon
TOC	Total Organic Carbon
TRU	Transuranic
USF	Uranium Solidification Facility
UT	Ultrasonic Testing
WAC	Waste Acceptance Criteria
WFE	Wiped Film Evaporator
WTP	Waste Treatment Plant

1.0 Introduction

The Defense Waste Processing Facility (DWPF) processes and vitrifies radioactive waste that it receives from the Concentration, Storage, and Transfer Facility (CSTF) and the Salt Waste Processing Facility (SWPF). The process involves feed preparation and a glass melter that eventually produces glass-filled canisters of stabilized waste. As a result of the evaporation of water during both the melter feed preparation and the melter feed vitrification steps in DWPF, a recycle waste stream is generated, neutralized, and sent back to the CSTF. The recycle waste is a dilute water stream originating from the collection of condensate liquids containing some minor sludge and frit solids and other waste components primarily resulting from entrainment into the condensate during foam-over events [1]. The recycle stream volume is significant and is expected to approach 3 million gallons per year once the SWPF reaches full operations. The recycle waste is currently collected in the Recycle Collection Tank (RCT) in DWPF, where corrosion inhibitors (i.e., hydroxide and nitrite) are added to the stream before it is transferred to the CSTF. In the CSTF, the waste is collected and stored in Tank 22 until it is transferred to the 242-16H (2H) evaporator where it is concentrated in order to conserve storage space or is utilized in salt batches.

Diverting the bulk of the recycle waste stream from the Tank Farm is essential for the eventual closure of the waste tanks, and hence the completion of the SRS liquid waste mission. Additionally, in the near term, ceasing recycle receipts to the Tank Farm will allow the CSTF to repurpose the 2H Evaporator as a general-purpose evaporator, operationally shut down the 242-25H (3H) Evaporator, and free up waste tanks currently dedicated to recycle receipt. Savannah River Remediation (SRR) recently performed a Systems Engineering Evaluation (SEE) for diverting the DWPF recycle stream [2]. Cross flow filtration and wiped film evaporation were selected as the preferred technologies for processing the recycle stream. The final streams produced from these unit operations, including filter solids, evaporator bottoms, and evaporator overheads, will be transferred to the sludge batch preparation tank, the salt batch preparation tank, and the Effluent Treatment Facility (ETF), respectively, with the ETF receiving the bulk of the recycle volume [3]. Transfer of much of the water from the DWPF recycle to ETF accomplishes the primary goal of diverting the bulk of the material from the CSTF.

The principal unit operations for the diverted recycle stream are the cross flow filters (CFF) and the wiped film evaporator (WFE). The equipment will be exposed to streams that contain a range of potentially corrosive dissolved species and abrasive undissolved species. Likewise, the transfer line piping between these unit operations will be exposed to these same environments. An evaluation was performed to assess the risk of erosion-corrosion to reduce the service life of these critical pieces of equipment and the associated transfer lines.

The diverted recycle stream is a dilute solution that contains anionic species such as nitrate, nitrite, hydroxide, sulfate, chloride and permanganate as well as oxidizing cations such as the ferric and

mercuric species [4]. The stream may also contain low levels (<10 wt. %) of undissolved solids such as metal oxides/hydroxides (i.e., sludge), monosodium titanate, or glass frit [4]. The evaporator concentrate product may also include other precipitated solids (Mn, Al, Si, Sodium Aluminosilicate (NAS), etc.). The compositional envelope for these potentially aggressive species and solids determined by other activities described in this plan were utilized for the corrosion/erosion-corrosion evaluation. Additionally, the CFF, and potentially the WFE, may be periodically cleaned with acid to mitigate pluggage. Thus, the materials of construction must be suitable in both caustic (pH 9 or greater) and acidic (pH 7 or less) environments.

Cross flow filters have been utilized extensively at this and other sites to handle caustic waste solutions. Corrosion testing has shown that the filter media can withstand a wide range of pH and contaminants without significant degradation [5]. The anticipated chemistry of the diverted recycle stream [6] was compared with the acceptable chemistry ranges observed with these tests in the filter media. However, the filter media testing was performed without the presence of the undissolved solids. The presence of these solids could potentially erode and/or corrode the sintered metal porous surface either opening or closing the pores and thus influence the performance of the cross flow filter. A literature review was performed to evaluate the plausibility of this mechanism.

The evaluation also assessed the influence of pH (i.e., expected feed range from 9-13) on the potential for corrosion and erosion in the WFE. The pH is expected to increase in the evaporator during evaporation. The baseline chemistry being developed for the RD process was utilized to evaluate the influence of pH [6]. The possibility that the undissolved solids in the feed may result in erosion in the WFE was also assessed. At present, the operating temperature of the WFE is anticipated to be approximately 60 °C [7]. To cover the range of possible scenarios, evaporator operational temperatures required for non-vacuum evaporation (>100 °C) were also considered.

The materials of construction (MOC) for the WFE have not been specified at this time. However, to ensure an extended life for the WFE, corrosion resistant materials (e.g., 304L stainless steel) and materials that provide both corrosion and erosion-corrosion resistance (e.g., Stellite) may be necessary. A literature review was performed to assess the various MOC options available.

A final consideration is the potential for NAS solids formation inside the WFE [2]. If these solids form, periodic cleaning utilizing an acid (e.g., nitric or oxalic) may be necessary. The resistance of the MOC to these cleaning acids was assessed.

The potential for corrosion and erosion-corrosion of transfer lines exposed to the current DWPF recycle stream has been previously reviewed [8]. The assumptions for that evaluation regarding chemistry and characteristics of the solids were reviewed and compared with the anticipated chemistry and solids for the diverted recycle stream. This evaluation determined whether a revision to the current baseline report is necessary.

2.0 Degradation Mechanisms

Material degradation limits the service life of engineered systems, structures and components. Material degradation either reduces the geometry of the stress bearing component such that it cannot sustain a load (referred to as the structural integrity), or penetrates through the material such that the component is no longer leak tight (referred to as leak integrity). Degradation mechanisms are qualitatively classified based on the factors involved and the change in the surface morphology that is produced. Table 2-1 shows common mechanical and chemical degradation mechanisms for engineered materials. Within each mechanism there may be several forms. Corrosion, for example, has at least 8 different types or forms (uniform, localized, galvanic, etc.) [9]. There is also the opportunity for synergism between these mechanisms (e.g., corrosion-fatigue) such that the rate of degradation is accelerated beyond that which would have occurred if there had only been a single mechanism.

Table 2-1 Chemical and Mechanical Degradation Mechanisms

Mechanical Degradation	Chemical Degradation
Fatigue	Uniform Corrosion
Creep	Pitting Corrosion
Overload	Environmentally Assisted Cracking (e.g., stress corrosion cracking (SCC))
Erosion	Galvanic Corrosion
	Microbiologically Induced Corrosion
	Crevice Corrosion

The initiation and rate at which degradation occurs depends on many factors related to the environment, applied and internal stresses, and material properties. Although the list is not comprehensive, Table 2-2 provides examples of each of these factors.

A literature review for the performance of MOCs for the transfer lines and the key unit operations for the Recycle Diversion (RD) process under various environments and conditions has indicated that there are at least four principal mechanisms of concern: corrosion [8], [10], erosion [10], [11], erosion-corrosion [12], and fatigue [13], [14]. A brief description of each mechanism is presented in the following sections.

Table 2-2 Environmental and Material Factors that Influence Corrosion

Environmental	Material
Solution Chemistry (e.g., contaminants, pH)	Grain size
Hydrodynamics	Heat treatment
Geometry of component	Impurities at grain boundaries
	Passive film characteristics

2.1 Corrosion

Corrosion is the destructive result of a chemical reaction between a metal or metal alloy and its environment [9]. Corrosion is the primary means by which most metals deteriorate on contact with water, acids, bases, salts, oils, and other solid and liquid chemicals [15]. Commonly, corrosion processes involve transfer of electronic charge between a metal and an aqueous environment. The metal dissolution process, or anodic reaction, involves dissolution of a metal species and release of a metal cation into the solution and the liberation of electrons in the metal. To maintain electroneutrality, the electrons in the metal are consumed by a cathodic reaction at the liquid-metal interface, which occurs at the same rate as the anodic reaction. Reduction of dissolved oxygen in the aqueous environment is an example of a cathodic reaction. If there is a deficiency of electrons at the metal surface, the interface between the metal and the solution becomes positively charged or anodically polarized. As the surface becomes more anodically polarized, the rate of corrosion increases (see Figure 2-1).

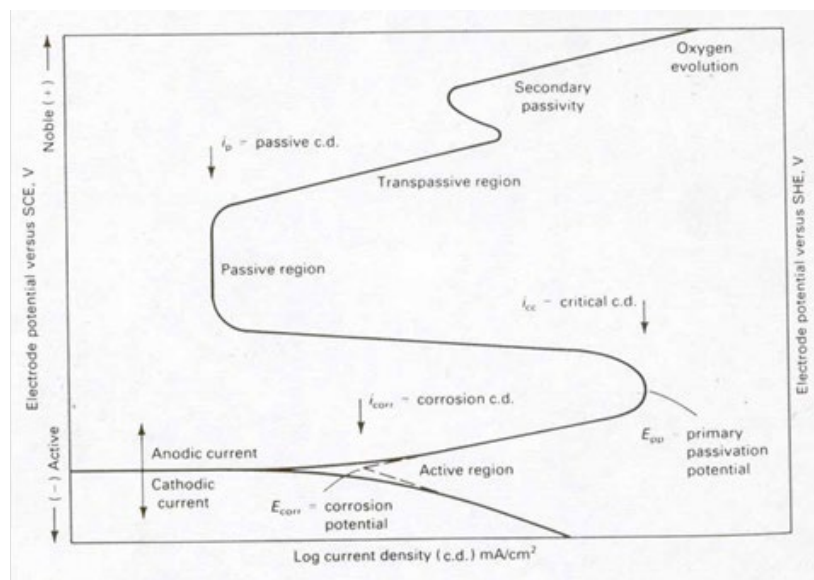


Figure 2-1 Potential vs. Current Diagram Illustrating Corrosion Behavior

In many engineering materials (e.g., aluminum, stainless steel alloys, etc.), the corrosion rate suddenly decreases above some critical potential, E_{pp} (see Figure 2-1). This corrosion resistance above E_{pp} is defined as passivity. Passivity is caused by formation of a thin, protective, hydrated oxide, corrosion-product surface film that acts as a barrier to metal dissolution. In many cases, the passive film exists naturally in aerated environments. Frequently alloying elements, such as chromium are added to a metal to increase the resistance of the passive film. Passive materials, however, are vulnerable to degradation as well. Because the passive film is thin and frequently brittle, mechanical or chemical breakdown may occur at local sites and result in localized corrosion of the underlying metal. These localized mechanisms are stochastic, depend on the local environments that evolve, and frequently occur at accelerated rates. Due to their random nature, the failure of a system by one of these mechanisms may be sudden and catastrophic. The breakdown of passivity is also illustrated in Figure 2-1. The increase in current shown in the transpassive region of the plot may be an indication of pit initiation and growth. Examples of localized corrosion include pitting corrosion, intergranular corrosion, de-alloying, and crevice corrosion. Localized corrosion may also act in concert with other factors such as stress and accelerate degradation. An example of this synergistic process is stress corrosion cracking (SCC).

Corrosion may be accelerated at a heat transfer surface [16], [17]. Two factors create greater concern at a heat transfer surface, such as the tube bundle for the evaporator or any heat exchanger surface that uses steam. First, the temperature at the heat transfer surface is greater than the bulk liquid temperature. Additionally, adherent deposits may form on the surface creating the opportunity for underdeposit or crevice corrosion. These deposits may cause accelerated corrosion during operation or during an outage if care is not taken to properly inhibit the solution. During operations, at the higher heat transfer surface conditions localized mechanisms such as pitting, SCC, or intergranular attack (IGA) [18] are the principal concern. In the latter case, during an outage, a failure beneath salt deposits on an evaporator tube bundle occurred due to pitting corrosion [19]. These corrosion mechanisms should be evaluated for the WFE.

Corrosion is managed by either materials selection (i.e., use of corrosion resistant materials such as stainless steels) or the addition of chemicals that inhibit corrosion for a given material/environment. For example, evaporation processes with high temperatures and corrosive solutions, the MOCs selected have been either stainless steel or nickel-based alloys. Both alloys depend on passivity to provide corrosion resistance and should be considered as candidates for the WFE MOCs. On the other hand, corrosion of stainless steel is accelerated by halide species (e.g., chloride). Addition of hydroxide, nitrite or nitrate inhibits corrosion of the material. Maintaining a system above critical concentrations of inhibitor or below critical temperatures provides protection against corrosion.

2.2 Erosion

Erosion is a form of wear that results in the progressive loss of the original material due to mechanical interaction between that surface and a fluid, multi-component fluid, or impinging liquid or solid particles [20]. For the unit operations in the RD process that handle flowing liquid (i.e., transfer lines, cross flow filters, and the vessel body of the WFE), the term slurry abrasive wear and erosion will be used synonymously. A slurry is defined as a liquid with entrained or suspended particles. The WFE blade is also subject to slurry abrasive wear as the viscous solution passes through the vessel.

The rate of degradation due to slurry abrasive wear is determined by the mechanical and physical characteristics of the solid particles, the slurry characteristics, and the properties of the metal surface. The significant erodent physical properties related to degradation are particle size distribution, particle shape (i.e., angularity), particle velocity, particle direction, and particle hardness. The critical slurry characteristics that influence degradation are temperature, flow rate, flow regime (i.e., laminar vs. turbulent), solids concentration, and slurry viscosity. The critical metal characteristics that influence degradation are temperature, roughness, hardness, and microstructural features (e.g., grain orientation). The individual effects of each variable are summarized in a comprehensive review by Duignan [21]. However, because of the number of variables and the manner in which these variables interact, prediction of erosion rates is extremely challenging if not impossible in some cases [22].

Abrasive wear may also occur as a hard, rough surface slides against a softer one, ploughing a series of grooves and removing material. This deterioration may be further accelerated when abrasive particles are introduced between the sliding surfaces, or when a part is moved through an abrasive medium (i.e., the WFE blade). Abrasive wear normally takes the form of a high-luster (i.e. semi-glossy) finish with a mirror-like surface structure. This type of wear may occur between a rotating shaft and the mechanical seals and bearings. This type of wear normally results in increased endplay or internal clearance, which can reduce fatigue life and result in misalignment. The primary causes of abrasive wear are: inadequate lubricant film formation; foreign particles (contaminants such as sand, fine metal from grinding, etc.) present in the lubricant; or insufficient lubricant. Furthermore, as the number of wear particles in the lubricant increases, this will further accelerate the abrasive wear process. Given that the WFE has a rotating shaft, the MOCs for the bearings, seals and shaft of the WFE should be carefully designed.

Slurry abrasive wear was observed on the 3H evaporator shell after 16 years of service [23]. This evaluation will review the failure analysis that was performed on the evaporator shell and determine its applicability to the RD process.

2.3 Erosion-Corrosion

Erosion-corrosion is defined as a corrosion reaction that is accelerated by the relative movement of the corrosive fluid and the metal surface [15]. An increase in the relative motion may increase corrosion by either removing protective films or increasing the diffusion or migration of deleterious species. In contrast, an increase in the fluid velocity can also decrease corrosion rates by eliminating aggressive anion concentration or enhancing passivation or inhibition by transporting the protective species to the fluid/metal interface. A review of this mechanism was performed by Imrich [12] as it pertained to the Hanford Waste Treatment Plant.

The spectrum of erosion-corrosion damage is shown in Figure 2-2. In stagnant conditions, corrosion dominates the damage mechanism and the rate decreases parabolically with time due to the formation and growth of the passive film. At low fluid velocities, flow assisted corrosion (FAC) is a function of the mass transfer rate of aggressive species and the protective film on the surface dissolves and corrosion continues at a roughly linear rate. Above a critical velocity, known as the breakaway velocity, the passive film is continuously damaged and removed. Thus, the overall degradation rate becomes a function of both the mechanical damage to the film and corrosion. At high fluid velocity, the metal removal process is controlled by cavitation erosion or by droplet impacts. The oxide is continuously removed and as a result, high metal losses occur due purely to erosion. The erosion process is time dependent and experiences an incubation period related to the time it takes for the surface to be embrittled.

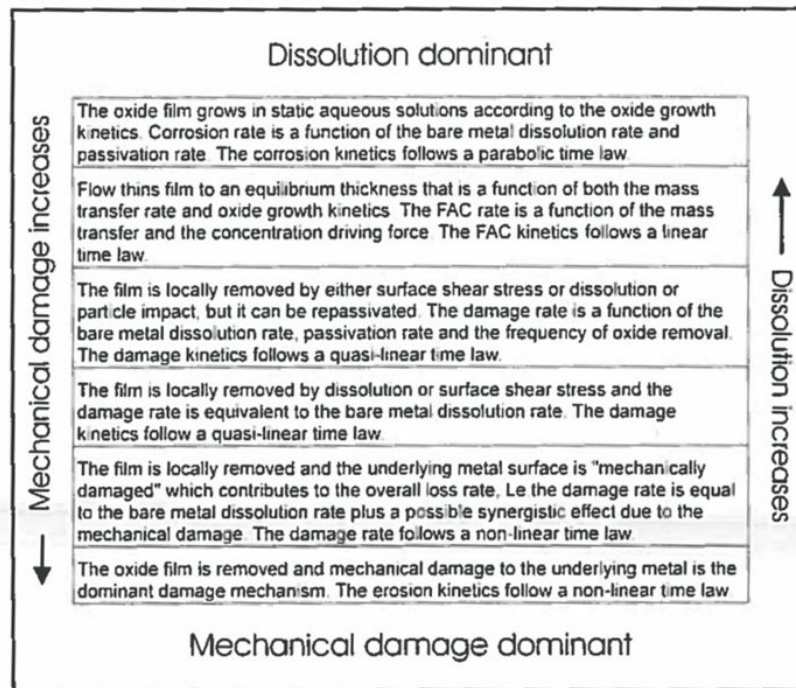


Figure 2-2 Spectrum of Corrosion and Erosion-Corrosion Behavior [15].

As mentioned previously, increasing the velocity can be beneficial in that it increases mass transfer of protective species, flushes crevices and suspends solids. However, eventually increasing the velocity results in turbulence that accelerates corrosion. Additionally, geometric irregularities, design features (e.g., elbows, orifices, flanges), and solid particles disrupt laminar flow and create turbulent conditions. It is this disturbed flow condition directly adjacent to the metal surface that must be considered when evaluating the potential for erosion-corrosion. These turbulent bursts can occur in discrete regions of the system (e.g., pipe elbow) and result in localized corrosion (e.g. pitting) of the system. These complex flow patterns form under the specific conditions of the system and the environment. Thus, data from tests performed under conditions that model the actual system are necessary to predict the actual degradation rates.

2.4 Fatigue

Fatigue damage of structures and components results from subjecting materials to fluctuating, or cyclical, stresses and strains. Failures are caused by the synergistic action of cyclical stress, tensile stress, and plastic strain. The cyclic stress and strain initiate the crack, while the tensile stress produces crack growth. Fatigue behavior and service life, which is difficult to characterize, is a function of stress level, stress state, cyclic wave form (i.e., amplitude and frequency), fatigue environment, and material microstructure (i.e., grain size, inclusions, etc.).

Fatigue stresses may be due to either vibrational or thermal cyclic loads. Turbulent flow through an elbow of a pipe results in a mechanical load on the system that must be supported adequately to allow for flexibility. Vibration created by a rotating shaft also creates a mechanical stress that requires materials with adequate properties to prevent overload of the system. Thermal expansion or contraction caused by temperature changes, acting against a constraint, may result in thermal stresses. Temperature gradients along and through the material, internal or external constraint, and numerous short heating and short cooling cycles are necessary for thermal fatigue to occur. An example of a thermal cyclic load occurs during the operation of the evaporators at SRS [19]. During operation of the evaporator, high temperature steam flows through the bent tube bundle. For outages, the steam to the tube bundle is turned off. Cold water is sent through the tube bundle for hydrotesting purposes in many cases. Additionally, deposits are removed from the surface of the tube bundle by intentionally thermally “shocking” the tube bundle [19]. The supports and the materials chosen for the tube bundle were specifically designed to address the possibility of thermal fatigue [24].

3.0 Literature Review of Transfer Line and Unit Operations in RD Environments

Degradation mechanisms for transfer lines, cross flow filters and wiped film evaporators were reviewed. In addition, corrosion testing and performance for the bent tube evaporator (BTE) at SRS were also reviewed and conditions that might apply to the WFE were evaluated.

3.1 Transfer Lines

Degradation of the stainless-steel transfer lines due to corrosion and erosion-corrosion was evaluated by Wiersma [8]. A thermal fatigue issue with a piping support associated with an evaporator was also reviewed. A summary of the key findings for each mechanism is discussed below.

3.1.1 Summary of Corrosion and Erosion-corrosion testing for SRS

The MOC for the tank farm transfer lines is 304L stainless steel. The lines are typically 3 to 4 inches in diameter and have wall thicknesses of schedule 10 or schedule 40 pipe. Testing of 304L stainless steel in simulated waste at representative temperatures was reviewed. Three principle corrosion mechanisms were considered: general, pitting and stress corrosion cracking.

Stainless steels exhibit general corrosion in strong acids or alkalis at high temperatures (e.g., greater than 100 °C). While stainless steels are utilized occasionally under these conditions, this is usually the exception rather than the norm. In most cases, the stainless steel is exposed to a passive environment with low general corrosion rates. The passive behavior is attributed to an adherent chromium oxide film that forms on the surface.

Testing on stainless steel coupons immersed in simulated waste solutions was performed to estimate the general corrosion rate. The five solutions used for the tests are shown in Table 3-1. The average general corrosion rates for each of the five solutions are summarized in Table 3-2. The general corrosion rate did not vary significantly with temperature between 30 and 60 °C, therefore only a single average corrosion rate was reported. The corrosion rates for the most part are significantly less than 0.1 mils/year (mpy). Given this corrosion rate and the typical pipe wall thickness, general corrosion would not be expected to cause failure or a leak for any reasonable service life [8]. Solution 4 (See Table 3-2) provides an upper bound general corrosion rate, 0.078 mpy, for stainless steel exposed to these solutions and conditions.

Coupon immersion tests with 304L stainless steel in simulated waste environments were also performed at Pacific Northwest Laboratory (PNL) for between 3000 to 4000 hours [25]. The compositions of the waste simulants are shown in Table 3-3. These compositions are similar to what are transported through the SRS transfer lines that service the high-level evaporator system. The chloride levels in solutions P-2 and P-4 are 2-10 times higher than what is typically present in

the SRS waste. The temperature for the tests was 60 °C. This temperature is at the lower bound of the temperature experienced in the gravity drain lines that leave the evaporator during operation; however, periodic evaporator shut-downs and the ground temperature would tend to moderate the temperature of these lines.

Table 3-1. Molar Anion Concentrations for Simulated Waste Solutions Tested at SRNL [26].

Solution Number	1	4	8	11	13
pH	13.7	13.6	12.7	12.4	12.5
OH ⁻	2.1	1.3	0.15	-	-
CO ₃ ⁼	0.1	0.16	0.098	-	-
NO ₂ ⁻	1.1	0.6	0.07	-	-
NO ₃ ⁻	1.4	2.0	0.7	-	4.6
Cl ⁻	0.022	0.022	0.0013	-	-
F ⁻	0.011	0.015	-	-	0.039
SO ₄ ⁼	0.095	0.14	0.0079	-	-
Al(OH) ₄ ⁻	0.3	0.31	0.007	-	0.26
C ₂ O ₄ ⁼	0.0051	0.014	-	-	-
CrO ₄ ⁼	0.0021	0.0033	0.00084	0.013	-
MoO ₄ ⁼	0.00027	0.00043	-	-	-
SiO ₃ ⁼	0.0021	0.0038	0.00058	-	-
PO ₄ ³⁻	0.0058	0.0085	0.014	0.22	-

Table 3-2. General Corrosion Rates for 304L Stainless Steel Exposed to Simulated Waste Environments at SRNL. Rates are in mils per year (mpy) [26].

Solution	Average Corrosion Rate (mpy)
1	0.010
4	0.078
8	0.015
11	0.001
13	0.035

The corrosion rates at these conditions are shown in Table 3-4. The rates were between 0.055 to 0.082 mpy, which are comparable to the maximum corrosion rates observed at SRNL, but still less than 0.1 mpy. At this corrosion rate, the stainless steel transfer lines would not experience significant degradation over an expected service life (e.g., less than 100 years).

Table 3-3. Molar Anion Concentrations for Simulated Waste Solutions Tested at PNL [25].

Solution Number	P-1	P-2	P-3	P-4
OH ⁻	10	10	10	10
CO ₃ ⁼	0	0	0	0.085
NO ₂ ⁻	1.36	1.36	1.36	0.2
NO ₃ ⁻	4.63	4.63	4.63	1
Cl ⁻	0	0.2	0	1
F ⁻	Saturated	Saturated	Saturated	Saturated
SO ₄ ⁼	0.05	0.05	0.05	0.05
Al(OH) ₄ ⁻	0.05	0.05	0.05	0.1
PO ₄ ³⁻	0.07	0.07	0.07	0.2

Table 3-4. General Corrosion Rates for 304L Stainless Steel Exposed to Simulated Waste Environments at PNL. Rates are in mils per year (mpy) [25].

Solution	Average Corrosion Rate (mpy)
P-1	0.055
P-2	0.082
P-3	0.055
P-4	0.066

Every engineering metal or alloy is susceptible to pitting, which is a highly localized form of corrosion that produces sharply defined holes in a material. Despite good resistance to general corrosion, stainless steels are more susceptible to pitting than many other metals. Pitting can be a destructive form of corrosion if it causes perforation of equipment. Pits may be isolated from each other on the surface or so close together that they resemble a roughened surface [27].

For stainless steel the most common cause of pit initiation is highly localized destruction of the passive film by contact with moisture that contains halide ions, particularly chloride ions [28]. Stagnant or low flow conditions favor the initiation and propagation of pits as well. The tendency for pitting also increases with increasing temperature and chloride ion concentration [29]. Inhibitors such as hydroxide, nitrate, chromate, sulfate and carbonate are added to a chloride bearing solution to reduce the pitting tendency. Although all these species are present, the two primary inhibitors that are present in waste solutions are hydroxide and nitrate. The literature indicates that a pH > 11 is sufficient to reduce the pitting tendency of stainless steel in seawater [29]. Given that the waste pH is typically much greater than 12 and the chloride concentration is much less than that of seawater, pitting in the waste transfer system under normal service conditions due to chlorides is not anticipated.

Electrochemical and coupon immersion tests at the conditions shown in Table 3-1 confirmed that at typical waste environment conditions, pitting corrosion of stainless steel would not be anticipated [30]. The coupons tested at PNL were also examined for evidence of pitting corrosion [25]. The coupons in simulants P-1 and P-4 were unattacked, while those exposed to simulants P-2 and P-3 exhibited only minor pitting. Overall, the performance of 304L at these conditions was described as excellent.

Stress corrosion cracking (SCC) is a general term describing failures that occur by cracking in corrosive environments under load [29]. The requirements for SCC are the presence of a tensile stress (i.e., either residual, applied or a combination of both), the presence of a specific corrodent, and a susceptible material. The cracks form at roughly right angles to the direction of the tensile stress at stress levels much lower than those required to fracture the material in the absence of the corrodent.

High level wastes at SRS are compatible with 304L stainless steel transfer lines and the sintered 316L CFF and will not cause SCC because they are dilute, basic, nitrate solutions, which contain incidental amounts of chloride and fluoride [31]. Stainless steels are most susceptible to stress corrosion cracking in solutions containing halide ions such as chloride. However, the presence of the nitrate ion in basic solution has been shown to prevent stress corrosion cracking by halides [32]. Laboratory testing was performed at SRS to confirm that 304L stainless steels were not susceptible to intergranular SCC in simulated waste environments [33]. The tests were performed in the same solutions (see Table 3-1) that were used for the general and pitting corrosion studies at a temperature of 60 °C. The samples were tested in the as-received condition and with a heat treatment designed to simulate the microstructure of a weld region. The slow strain rate or constant extension rate test was utilized to determine SCC susceptibility [34]. The results of the tests showed that 304L, even in the heat treated or welded condition was not susceptible to SCC [33].

Transgranular SCC is a problem for 300 series stainless steels exposed to solutions that are neutral or acidic (pH 2-8). As mentioned previously, increasing the pH or adding nitrate ions to a solution decreases the tendency for stress corrosion cracking by chloride [32]. Under normal service conditions at SRS, transgranular SCC is not anticipated. However, if natural water (e.g., well water or ground water), which has a neutral to slightly acidic pH, is allowed to contact the stainless steel for an extended period of time (e.g. several months), problems could arise such as microbially influenced corrosion (MIC).

Instances of transgranular SCC have been observed in the waste tank farm. In each case natural water was involved and the chloride ion was observed to be the species that initiated the attack. Stress corrosion cracking of a stainless steel core transfer line was also observed [35] near a clean-out port in the concentrate transfer system (CTS) loop for Tanks 29-32 in the early 1980's (See Figure 3-1). The piping had been placed according to the revision of Specification 4482 applicable at that time. The failures at the clean-out port probably occurred sometime between hydro-testing

of the system and placing the line in radioactive service. Natural well water, with no added corrosion inhibitors, was utilized for the hydro-test and is the likely source of the chloride ions. Although the well water is typically low in chlorides (less than 5 ppm), evaporation may have increased the chloride concentration. Concurrent with this failure, it was discovered that an underground steam line near the clean-out port had leaked for an extended period. During the repair of the steam line, the degree and extent of heated soil in the area was observed to be unusual. The steam leakage was postulated as a heat source which would produce the elevated temperatures necessary to enhance stress corrosion cracking. A time/temperature combination is also required for cracks to initiate and propagate. It was observed that both the extended period of steam leakage and the extended period before the line was placed in service were likely contributors to the failure. It was therefore recommended that the repair time for leaks in buried steam lines be minimized and that new pipelines should not be held out of service for extended periods of time [35].

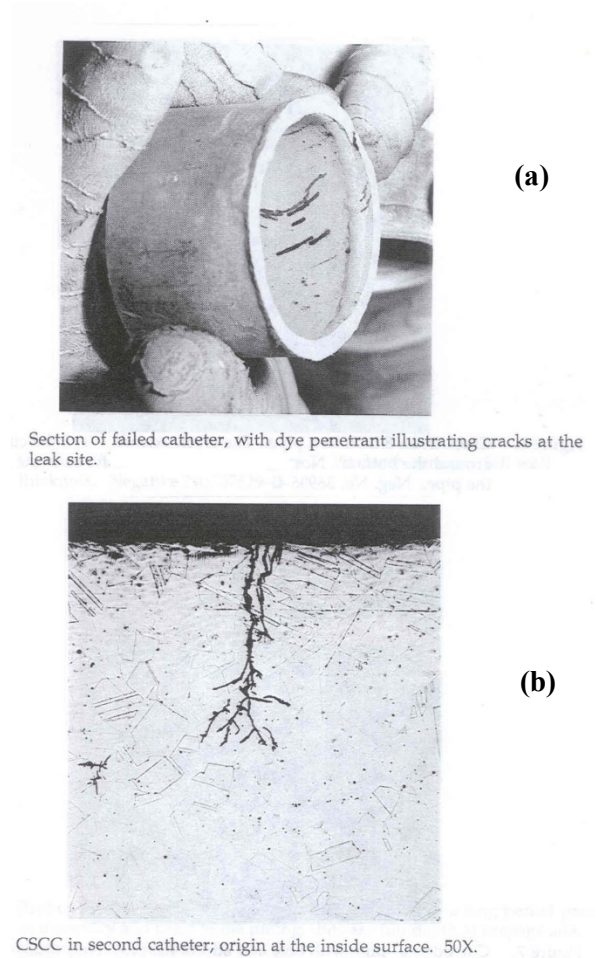


Figure 3-1. Section of core pipe from clean-out-port #3: (a) Dye penetrant test showing cracks on the interior of the pipe, (b) Micrograph showing transgranular chloride SCC [35].

Due to this failure, it was also recommended that the time for which the transfer lines are exposed to stagnant well water at elevated temperatures be minimized. Administrative controls, such as the Corrosion Control Program Description Document, are in place to minimize the potential for well water to be left in the lines for extended periods of time [36]. In fact, placing the lines in service with the waste supernate, which contains inhibitors such as nitrite and hydroxide, will protect the stainless steel.

3.1.2 Corrosion Testing in Support of Glycolic Acid Flowsheet

Savannah River Remediation (SRR) plans to utilize glycolic acid to replace the formic acid as an alternate reductant for the Defense Waste Processing Facility (DWPF) at Savannah River Site (SRS). Glycolate, which is the product that may remain after using glycolic acid, can also be carried downstream to High-Level Waste and Low-Level Waste facilities. Testing has been done to perform a corrosion assessment for the components of the DWPF facility and other waste facilities that would be exposed to glycolic acid/glycolate [37].

Electrochemical corrosion tests were utilized to assess the impact of the DWPF nitric-glycolic acid flowsheet for the CSTF transfer lines that were constructed of 304L stainless steel [37]. The simulants utilized for the electrochemical tests are shown in Table 3-5. The pH for the simulants ranged from 8 to 13, while tests with no glycolate and 10,000 ppm glycolate were performed. No mercury was added to these test simulants. The test temperature was typically at 30 °C. In all cases the corrosion rates were on the order of 0.1 mpy or less with no susceptibility to localized corrosion. These results are similar to those found previously for 304L in simulated waste solutions. Therefore, the glycolate anion will not influence corrosion of the transfer lines in the CSTF. It was also noted that all four solutions were outside the chemistry control limits for the CSTF infrastructure [38], [36].

Complete oxidation of glycolate and other organic species from the SRAT may be necessary to minimize thermolytic hydrogen generation [39]. The glycolate oxidation may occur in the Recycle Collection Tank (RCT). The RCT receives material from the contents of the Slurry Mix Evaporator Condensate Tank (SMECT), the Off-gas Condensate Tank (OGCT), and a variety of lower volume feeds. The RCT heel would be adjusted with sodium hydroxide, to maintain the solution caustic, and sodium nitrite, a corrosion inhibitor prior to the addition of condensate and other feeds. The RCT collects the waste to be transferred via the Low Point Pump Pit – Recycle Pump Tank (LPPP-RPT) through a jacketed transfer-line to the Tank Farm facility. Scoping studies were performed to evaluate sodium permanganate and Fenton's reagent (i.e., iron catalyzed hydrogen peroxide) for destroying the glycolate. From the results of testing, oxidation by sodium permanganate was chosen over Fenton's reagent [40].

Electrochemical corrosion tests were used to evaluate 304L stainless steel with an RCT simulant that contained permanganate [41] and a RCT simulant that was blended with a Slurry Receipt

Adjustment Tank (SRAT) simulant (SB9-NG [42]). The composition of the RCT simulant is shown in Table 3-6. One set of electrochemical tests were performed with the RCT Simulant that contained the maximum level of permanganate and no glycolate. The maximum level was at a concentration where the molar ratio of permanganate to glycolate was 7¹ or approximately 0.002 M. No mercury compounds were added to the simulant. The tests were conducted at 25 °C. The hydroxide concentration was 0.1 M and the corrosion inhibitor nitrite was added such that the molar concentration ratio of the nitrite/nitrate was greater than 1.66 [36].

Table 3-5 Simulant Compositions for Glycolic Acid Flowsheet Testing for 304L [37].

	Acidic Recycle (pH 8) (M)	Basic Recycle (pH 11.5) (M)	Basic Concentrated Recycle (pH 13) (M)	Salt Solution Simulant (pH 13) (M)
Sodium Hydroxide	NA	0.1	0.01	0.01
Sodium Carbonate	NA	NA	0.45	0.26
Aluminum Nitrate	1E-03	3E-05	NA	NA
Iron Nitrate	5E-04	4E-05	NA	NA
Manganese Nitrate	3E-04	NA	NA	NA
Sodium Glycolate	0.16	0.16	0.13	0.13
Sodium Fluoride	1.26E-03	NA	NA	NA
Sodium Chloride	1.7E-04	NA	NA	0.01
Sodium Nitrite	NA	0.11	1.66	0.61
Sodium Nitrate	0.031	0.09	1.06	2.44
Sodium Sulfate	7.6E-04	6E-04	0.02	0.09
Sodium Phosphate	NA	NA	4E-03	0.01

A second set of electrochemical tests utilized the RCT simulant, blended with the SRAT simulant. The tests were conducted three hours after addition of permanganate. The SRAT simulant was trimmed with low levels of mercury (~2.48 ppm) [42]. The level after 3 hours was not measured, but it is likely that the glycolate level had decreased to on the order of 10 ppm or less [43]. The hydroxide concentration was 0.1 M and the corrosion inhibitor nitrite was added such that the molar concentration ratio of the nitrite/nitrate was greater than 1.66 as shown in Table 3-6 [36].

¹ At the time of the experiments, the recommended molar ratio of permanganate to glycolate was 7. Later experimentation determined that the optimum ratio was 5.7 [43].

The electrochemical tests measured the instantaneous corrosion rate and localized corrosion susceptibility. For the RCT simulant with permanganate, the measured corrosion for 304L was 0.29 mpy. No susceptibility to localized corrosion was observed at these conditions. The corrosion rate for 304L in the RCT simulant with the SRAT simulant, was also low at 0.32 mpy. Again, no susceptibility to localized corrosion was observed.

The results of this corrosion study using RCT simulants with permanganate (no glycolate) and with SRAT component (includes glycolate) showed that accelerated general corrosion and localized corrosion is not expected for the stainless steel transfer lines exposed to the residual permanganate or mercuric ion at pH 13.

Table 3-6. Recycle Collection Tank (RCT) Simulant Composition [41].

Component(s)	Source	Formula	Concentration (M)	Final Concentration with addition of SRAT sludge (M)
Formate	Sodium Formate	Na(CHO ₂)	0.004	0.009
Oxalate	Sodium Oxalate	Na ₂ C ₂ O ₄	0.00022	0.00042
Nitrate	Sodium Nitrate	NaNO ₃	0.050	0.051
Nitrite	Sodium Nitrite	NaNO ₂	0.220	0.220
Hydroxide	Sodium Hydroxide (50wt% solution)	NaOH	0.10	0.10
Glycolate, formate, oxalate, nitrate	SRAT product (SB9-NG)	N/A	2.20 g per 1000 g Reagent Portion	N/A

3.1.3 Erosion-Corrosion

Early in the DWPF process development, the abrasive effect of both glass frit and sludge on process equipment and piping was addressed. Compared to the SRS sludge, the DWPF frit has a larger particle size and is more abrasive. Laboratory studies performed to assess the erosion resistance of 304L stainless steel included three separate erosion test loops and the Miller Abrasivity Test [44]. The piping for the test loops contained both straight sections and elbows. The fluid velocities tested ranged between 3 to 20 feet/s. The fluid was circulated through the pipes from 200 to 1350 hours. The wt. % solids for the slurries utilized in the tests tended to be very high (~ 40 wt.%) compared to that of the feed stream to DWPF (~ 10 wt.% [45]) and the DWPF recycle stream (~ 0.14 wt. % [46]) that are being sent to the tank farm. Post-test ultrasonic thickness measurements of the piping indicated no wall loss due to erosion.

Field experience in the DWPF was also utilized to assess the potential for erosion-corrosion due to the frit [47]. The Slurry Mix Evaporator (SME) permanent sample line system and the canister decontamination system handle solutions containing approximately 40 wt.% and 8 wt.% frit, respectively. Both systems are constructed of Hastelloy C276, an alloy that is expected to have

similar erosion-corrosion resistance to stainless steel. No significant wall thinning, or erosion of the components was observed after 1 year of operation.

During the initial period of operation of DWPF, foaming occurred in the slurry mix evaporator (SME). As a result, frit became entrained in the overhead stream that was sent to the recycle collection tank (RCT). The contents of the RCT were then pH adjusted to greater than 12 and then recycled back to the tank farm. The average solids carry-over was expected to be approximately 0.14 wt.% (0.09 wt.% frit + 0.05 wt. % sludge solids) [46]. The actual frit carry-over since the facility began operating has been monitored. The concentration of lithium was initially (i.e., late 1990's early 2000's) used to estimate the amount of frit solids carry-over and the concentration of iron was used to estimate the amount of sludge carry-over. In most cases, the levels of lithium were below detectable amounts (less than 30 ppm) indicating frit carry-over is small [48]. During the initial stages iron levels were also frequently below detectable (less than 200 ppm) indicating sludge carry-over was also small. Currently the levels of frit carry-over are lower since foaming in the SME is being controlled. If foaming is kept under control, frit carry-over is insignificant.

Tests performed on slurries of "fresh" glass frit (i.e., large particles with sharp-edged corners) indicated that the frit is more abrasive than the pure white silica sand utilized for the standard Miller tests [44]. However, the frit that the tank farm transfer lines are exposed to likely will not be "fresh". As part of the DWPF process, the frit is agitated with an impeller in the slurry mix evaporator (SME). As a result, the glass particles are broken up and the edges of the particles become more rounded. These smaller, rounder particles are likely more representative of much of the frit carry-over to the tank farm. Tests were also performed on glass frit which had been agitated with an impeller. Slurries that contained frit which had been agitated were much less abrasive [44].

Frit carry-over from the DWPF recycle stream is not expected to be an erosion-corrosion concern for the waste transfer lines. This conclusion was based on the relatively small amount of frit carry-over, the low fluid velocity (i.e., less than 5 ft/s), and the minimal amount of erosion-corrosion observed in DWPF systems that had significantly more frit compared to frit carry-over to the tank farm. The erosion rate is likely between the general loss rate for stainless steel in high level waste (0.078 mpy) and that indicated for the sludge slurry (0.4 mpy [49]). The rate was conservatively assumed to be 0.2 mpy. The low usage of the transfer lines associated with the DWPF recycle stream reduces the possibility for significant erosion-corrosion of the piping. [Note: Usage is a function of the frequency of transfers and the time it takes to make a transfer.] Usage factors, which estimate the time the pipe is exposed to flowing sludge slurry, were determined to estimate the actual wall loss for a given period. The erosion-corrosion degradation predicted was considered negligible for any reasonable anticipated service life (e.g., less than 100 years).

PNL constructed flow loop systems to study the effects of erosion-corrosion on the stainless steel transfer lines at Hanford [25]. The compositions of the simulants utilized for the tests are shown in Table 3-7. The compositions of these simulants are similar to the wastes at SRS. However, there was not extensive detail on the undissolved solids concentration. The operating conditions for the tests were 170 °F (~77°C) at flow velocities ranging from 3.3 to 9.3 ft/s. The system was frequently shut down, drained, flushed with distilled water and lay-ups were alternated between wet and dry (i.e., representative of what occurs in the field). The test run times ranged between 85 and 1100 hours (Note: tests were typically stopped due to problems with the pumps or pluggage in the test line). No evidence of erosion-corrosion was observed on the samples.

Table 3-7. Molar Anion Concentrations for Simulated Waste Solutions Tested at PNL [25].

Solution Number	P-5	P-6
OH ⁻	7	10
CO ₃ ⁼	0.09	0
NO ₂ ⁻	4.1	2.6
NO ₃ ⁻	1	1
Cl ⁻	1	0.2
F ⁻	Saturated	Saturated
SO ₄ ⁼	0.05	0.05
Al(OH) ₄ ⁻	0.5	0.2
PO ₄ ³⁻	0	0

3.1.4 Thermal Fatigue

Low cycle, high stress thermal fatigue was identified as the cause of leakage in the stainless-steel core pipe of one high level waste transfer line. Transfer line # 501, which is near the 1H evaporator, failed in a straight, anchored section of the core pipe. The combination of anchoring the internal pipe to the jacket, restricting the space for expansion, and having multiple lines within the same jacket intensified the stresses on the transfer line. The line had been in service for approximately 4.5 years and had experienced approximately 5500 thermal cycles [50]. The cycles resulted from transfer of concentrated waste from the evaporator at 115-135 °C alternated with desalination backflushes with water at 20-50 °C. The 502 transfer line, which is adjacent to the 501 line in the same carbon steel jacket, also showed indications of cracks at the anchor plate between the jacket and the core pipe. This second line had been in service for only six months and had experienced approximately 100 thermal cycles.

Piping flexibility analyses are routinely performed on new transfer lines [51]. Thus, any piping that has been designed and installed since 1980 has also been analyzed for thermal fatigue concerns.

3.2 Cross Flow Filters

3.2.1 SRNL Corrosion Testing for LAWPS Cross Flow Filter Materials

SRNL performed corrosion testing to support the Hanford Low Activity Waste Pretreatment System (LAWPS) project [52]. The key process operations for treating the waste include solids filtration and cesium removal. The planned method for solids separation was CFF. The MOC for the filter is sintered (i.e., porous) 316L stainless steel.

The fabrication of the sintered metal filter media results in a crevice-like structure having numerous small contact points (see Figure 3-2). There was a concern that the localized corrosion resistance of the CFF may be reduced as the pH of the solution is cycled between the well inhibited high pH waste feed chemistry to that ultimately of the planned cleaning acid chemistry. This would be further exacerbated when aggressive anions, such as chloride and sulfate, are present. Conditions like these can result during the proposed acid cleaning cycle or during extended outages if proper layup procedures are not followed. Corrosion of small contact points could result in the opening of the filter's effective pore size or potentially impact the structural integrity of the filter, which may increase the filter tube replacement frequency.

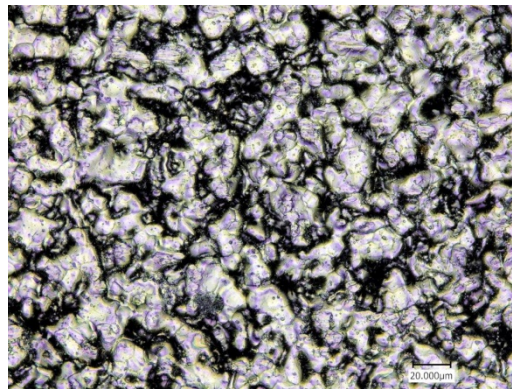


Figure 3-2. Sintered 316L material at 1000X magnification [52].

Electrochemical corrosion testing was performed to evaluate the corrosion resistance of Type 316L (316L) stainless steel, grade 0.1 Mott² crossflow filter media material in the anticipated chemistries and conditions of LAWPS service. Two series of electrochemical tests were performed. In the first test series, three test solutions were used: an alkaline 2M sodium nitrate solution (pH ~13), which was used as a simplified high level waste simulant; a neutral 2M sodium nitrate solution (pH 7); and 0.45M nitric acid solution, a potential cleaning solution for the filter (pH 0.7). The simulant recipe for the second set of testing was based on the 5 wt.% undissolved solids Pretreatment Engineering Platform (PEP) simulant, which was developed during scaled testing of Hanford Waste Treatment Plant (WTP) pretreatment processes [53]. The simulant was

² Sintered metal cross flow filters are manufactured by the Mott Corporation.

developed to mimic specific characteristics of the Hanford waste including solids and chemical components. The supernate was a 5M Na solution containing principally sodium salts at concentrations within the ranges expected for waste feeds to the WTP. The solids included aluminum and iron oxides as well as oxalate. A master batch of the PEP simulant was made for all testing and the concentrations of principal components are given in Table 3-8. The specific gravity for the simulant was approximately 1.23 and the pH was 13.4. For the first test series, tests were performed at 30 °C. Test temperatures for the second series were at 25 or 45 °C, with the testing focusing on the higher temperature since corrosion is more aggressive at these conditions.

Table 3-8. Chemical Analysis for Master Batch of PEP Supernate [52].

Element	Al	Fe	Na	NO ₃ ⁻	NO ₂ ⁻	Cl ⁻	SO ₄ ⁻²
Concentration*	5455	0.3	108000	110500	20900	<100	15700

* Concentration in mg/L

When more aggressive corrosion conditions were simulated, measured quantities of sodium chloride and sodium sulfate were added to the pH adjusted simulant to reach the desired soluble concentrations of these species. Target chloride concentrations ranged from 100 to 40,000 ppm. The original sulfate concentrations for the master batch of the PEP supernate were utilized.

The electrochemical test results indicated that the 316L crossflow Mott filter was resistant to localized corrosion for a representative alkaline low activity waste (LAW) simulant and to the anticipated cleaning acid solutions of 0.45M nitric acid and 0.45M oxalic acid. Tests performed in simulants with a pH 13 showed excellent corrosion resistance. A reduction in resistance was observed in a neutral pH solution, which was created by the mixing of simulant with the cleaning acid. The neutral pH condition will exist in the filter during the cleaning process (high pH to low pH) and during the return to normal operating conditions (low pH to high pH). Cleaning with the oxalic acid solution appeared to result in a less corrosion resistant material compared with the nitric acid. Corrosion resistance also decreased as the temperature was increased from 25 to 45 °C. Additional reduction in resistance was observed as the chloride concentrations increased for the crevice-type environment within the pores of the filter as would be expected during the first part of the cleaning process (high pH to low pH). The most aggressive solution was a mixture of the LAW simulant with oxalic acid at a neutral pH and chloride and sulfate concentrations of 40,000 ppm and 15,000 ppm, respectively. It should be noted however, that for the tests performed at the neutral pH with 10,000 ppm chloride at 45 °C, there were no indications of susceptibility to accelerated attack or localized attack.

3.2.2 Flow-through Tests for Hanford LAWPS Cross Flow Filters

A flow through test with the sintered metal material was performed to confirm the results of the electrochemical tests. The experimental set-up for the tests is shown in Figure 3-3. The length of the tube was 3 inches, the inside diameter of the tubes was nominally 0.5 inch, and the outside

diameter was nominally 0.625 inch. The filter media was 0.1 μm grade. The most aggressive environmental conditions as determined from the electrochemical tests were selected for this test. The test was designed to look principally at corrosion and therefore no undissolved solids were added initially. The test temperature was approximately 45 °C.

Both axial flow through the filter and perpendicular flow through the porous media was achieved. The axial velocity was 2-3 ft/s, while the transmembrane pressure was on the order of 30 to 45 psig. The test was conducted for 1 month. During that time the pH of the simulant ranged from 7 to 9 and precipitation of oxalate occurred. The oxalic acid cleaning cycle was also simulated.

Following the tests, the filter media sections were removed and examined for evidence of corrosion. Figure 3-4 shows the CFF samples after they had been removed from the system and cleaned. Results of the filter characterizations, water permeability, gas permeability and bubble point, following the filter flow through test were inconclusive. Two of the three filter tubes showed no significant increase in pore size or permeability as compared to the three as-received untested tubes. Although the chemistry tested was high in chloride and sulfate concentration and maintained at a relatively low pH (<10) for one month, evidence of significant localized corrosive attack, pitting or crevice corrosion, was not observed within the resolution of the various filter characterization test methods. This conclusion was also verified by the filter flow rates tests, which indicated no significant change in flow rate had occurred during the flow-through test. The third exposed filter tube, on the other hand, demonstrated a significant increase in pore size, exhibiting an increase of approximately 2 times in pore size as compared to all the other tube samples. Although brown colored deposits were observed on all surfaces of this filter, no plausible explanation could be postulated that would explain a corrosion mechanism that would have affected the entire wall thickness. Testing showed the range of pore size was much broader for this one sample demonstrating a broader effect. Based on the electrochemical testing, it seems unlikely that the increase in pore size resulted from a localized corrosive attack. Further testing of this tube would be required to determine the cause and extent of the increased pore size.

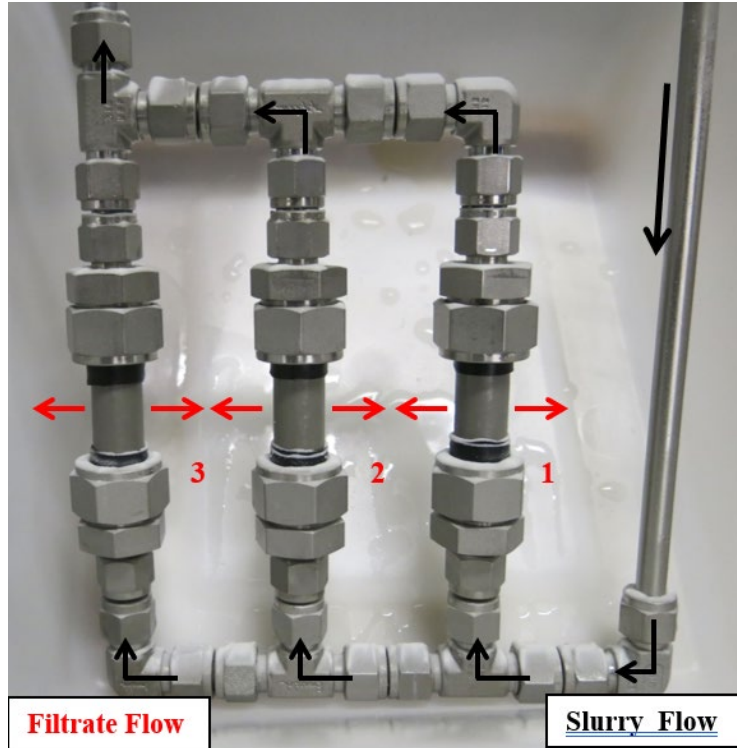


Figure 3-3. Set-up for CFF flow through tests [52].



Figure 3-4. Post-test CFF filter media samples after cleaning [52].

3.3 Wiped Film Evaporator Corrosion and Erosion-Corrosion Testing

3.3.1 SRL Testing (1975-1982)

Two WFEs were tested at the Savannah River Laboratory (SRL) in the mid-1970s to demonstrate their efficiency for handling liquid waste [13], [54]. One unit was horizontal with 10 ft² of heat transfer surface (see Figure 3-5), and the second unit was vertical with 5 ft² of heat transfer surface (see Figure 3-6). Both evaporators were constructed of 304L stainless steel. Three concentrated simulated wastes were tested in each evaporator.

- Solution 1: 2.7 M NaOH, 1.9 M NaAlO₂, 2.5 M NaNO₃, 1.7 M NaNO₂, 0.2 M Na₂CO₃, 0.02 M Na₃PO₄
Solution 2: 5.5 M NaOH, 1.4 M NaAlO₂, 2.7 M NaNO₃, 2.0 M NaNO₂, 0.08 M Na₂CO₃, 0.01 M Na₃PO₄
Solution 3: 5.5 M NaOH, 3.0 M NaAlO₂, 2.0 M NaNO₃, 3.0 M NaNO₂

The steam pressures were between 24 psig and 140 psig (i.e., 265 °F (~129°C) and 361 °F(~183°C)), while the feed rates were between 0.1 and 0.7 gpm.

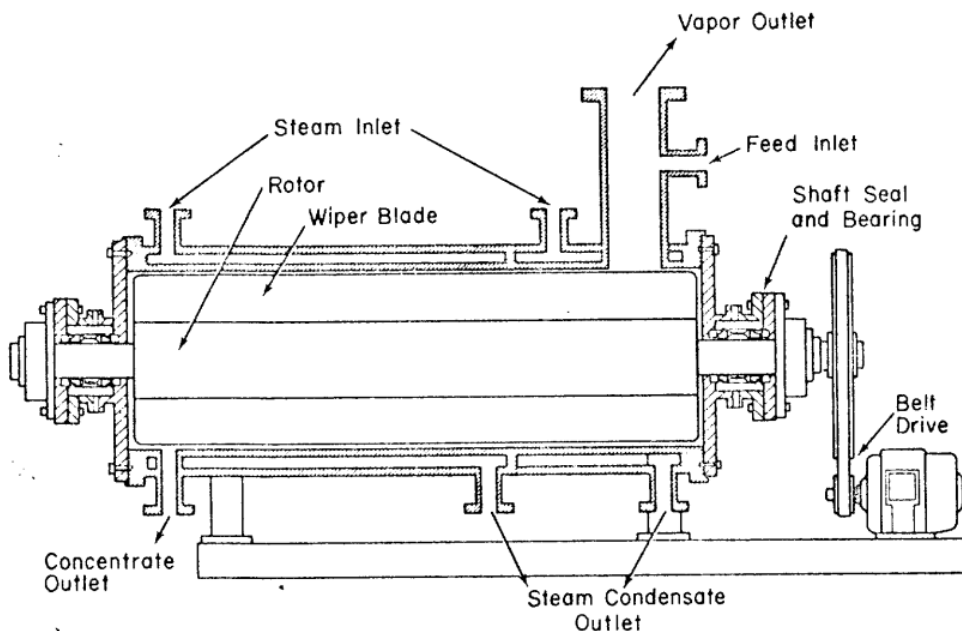


Figure 3-5. Schematic of Horizontal WFE [13].

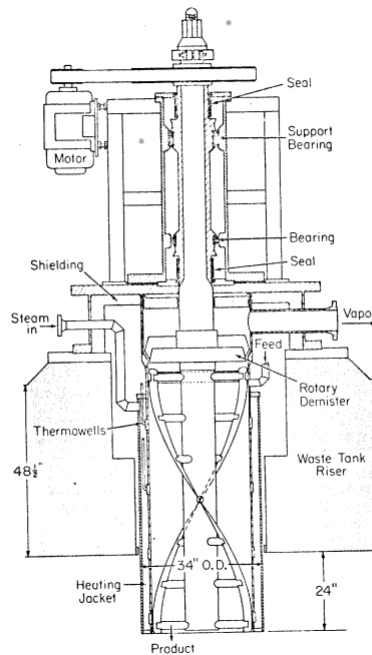


Figure 3-6. Schematic of Vertical WFE.

The horizontal WFE was operated for 2093 hours, of which 1741 hours were intermittent operation and 352 hours were continuous. Operation was interrupted occasionally to change various experimental parameters (e.g., steam pressure, feed rate, solution chemistry, etc.). The unit was disassembled for inspection. No bearing or mechanical seal failures were observed (i.e., abrasive wear was not an issue). However, three areas of concern were raised:

- 1) Six rotor blade support posts (at the outlet end) had fatigue cracks adjacent to the welds between the support posts and the rotor. The fatigue cracks are shown in Figure 3-7. The fatigue cracks likely occurred when the steam pressure was raised to determine the maximum operating temperature (i.e., thermal fatigue). This failure suggested that future evaporators should be designed to support the blades in such a manner that thermal fatigue is minimized.
- 2) The grease in the rotor bearing at the product outlet had begun to degrade, likely due to increased test temperatures. Although there was no indication of abrasive wear at the completion of the tests, degradation of the grease could potentially have led to a problem. High temperature grease or improved bearing materials should be investigated to address this problem.
- 3) Two sets of mechanical seals were installed on the evaporator. One set used a carbon rotating ring and a 17-4 PH stainless steel stationary ring and the other set mated tungsten carbide rotating and stationary rings. The inspection showed no appreciable abrasive

wear on the carbon-stainless steel combination. However, there was significant wear on the tungsten carbide-tungsten carbide couple. This couple should be avoided in future WFE designs. An alternative seal constructed of a carbon rotating ring and a tungsten carbide stationary ring was proposed as the best available combination.



Figure 3-7 Large fatigue striations with finer secondary striations perpendicular to the primary striations [14].

The vertical WFE was operated for 1111 hours with two problem areas identified.

- 1) The mechanical seals originally installed in the evaporator were composed of a tungsten-carbide rotating ring and a stationary tungsten carbide rotating ring. The seals had leakage problems and were modified to use a carbon rotating ring and a tungsten-carbide stationary ring. The initial indication was that this change was effective. However, it is unknown as to how long the WFE was tested with this implemented change.
- 2) Solids build-up in the discharge head of the evaporator resulted in contact with the blades that bent the tips. The tips were straightened, the discharge head was re-designed to eliminate solids build-up and the unit was returned to service. The problem seemed to be eliminated by the re-design.

The problems with the tungsten-carbide materials may have been related to corrosion. In 2000, Savannah River Technology Center (SRTC) performed tests to isolate the cause of slurry pump shafts “sticking” during start-up for waste retrieval [55]. Tests in simulated wastes revealed that the tungsten-carbide coating on the shaft was corroding and corrosion products were building up in the gap between the shaft and the bearing. This resulted in the shaft binding. The leaking that was observed for the vertical WFE may also have been due to exposure of the tungsten-carbide to the simulated waste. These observations suggest that tungsten carbide materials for the wetted parts of the WFE should be avoided for liquid waste applications.

It is important to note that the internal components showed no evidence of corrosion or wear after 2093 hours of operation for the horizontal WFE and for up to 1111 hours for the vertical WFE. The beneficial qualities of the passive film are the likely reason for the excellent performance. The lack of corrosion is a good indicator of a robust MOC, as this test would also simulate a “hot wall” corrosion test [13].

3.3.2 SRL Testing for the Uranium Solidification Facility (1988-1989)

In 1988, the Savannah River Laboratory performed corrosion tests in support of the Uranium Solidification Facility (USF) [56]. Uranyl nitrate in a nitric acid solution was concentrated by a series of three evaporators for subsequent conversion to an oxide powder in the USF. The purpose of the solidification was to produce a transportable form of uranium for safe shipment to Oak Ridge. The third evaporator in the series was to be a WFE. The plans were to construct the WFE of 6-inch diameter, schedule 40, 304L stainless pipe.

Corrosion tests were performed with 304L stainless steel plate in a simulated USF environment. The metallurgical conditions of the weld heat affected zone were reproduced by heating the coupons in air for 4 hours at 650 °C. This produced a sensitized microstructure (see Figure 3-8) that exhibited chromium carbide precipitates at the grain boundary. The coupons were partially immersed in the test solutions to show the effects from exposure to both vapor and liquid. The test solutions were selected to address the high-acid range of mixtures expected in the WFE. The solution compositions are shown in Table 3-9. The solution temperature was approximately 115 °C and the tests were conducted for 230 hours.

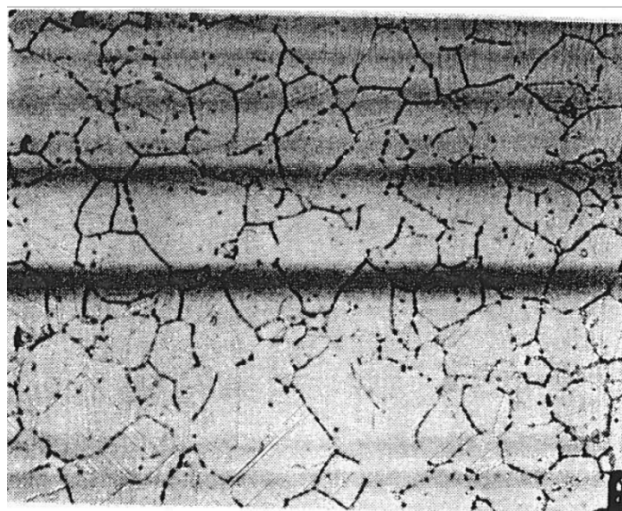


Figure 3-8. Optical micrograph of sensitized 304L stainless steel microstructure (500 X magnification) [56].

Table 3-9. Solution Compositions for 304L Exposure Tests [56].

Solution	Uranyl Nitrate (wt.%)	Nitric Acid (wt.%)	Chloride Ion (mg/l)	Dichromate (VI) (mg/l)
A	50	29	30	5
B	50	23	30	5
C	63	17	30	5
D	63	13	30	5

Figure 3-9 and Figure 3-10 are scanning electron microscope (SEM) images that illustrate the extensive intergranular attack (IGA) that occurred during the test. Most of the grains at the surfaces had dropped away in both vapor and liquid exposed metal surfaces. The depth of intergranular attack was measured from the SEM image shown in Figure 3-10. The rates of attack in both the liquid and vapor space for each solution are shown in Table 3-10. The corrosion rates were similar for the liquid and vapor space and ranged from 80 to 140 mils/yr. Assuming a nominal wall thickness of 0.28 inches for the 6-inch diameter pipe, failure due to IGA would occur within 6 years. This service life assumes continuous usage, which is likely conservative. Another consideration that was mentioned was that the evaporator bottoms would tend to accumulate constituents of the stainless steel (e.g., iron, chromium, and nickel). The concentration of these species could reach unacceptable levels for downstream processes. No further documentation on testing for this WFE was located. However, the process and equipment were never placed in service.

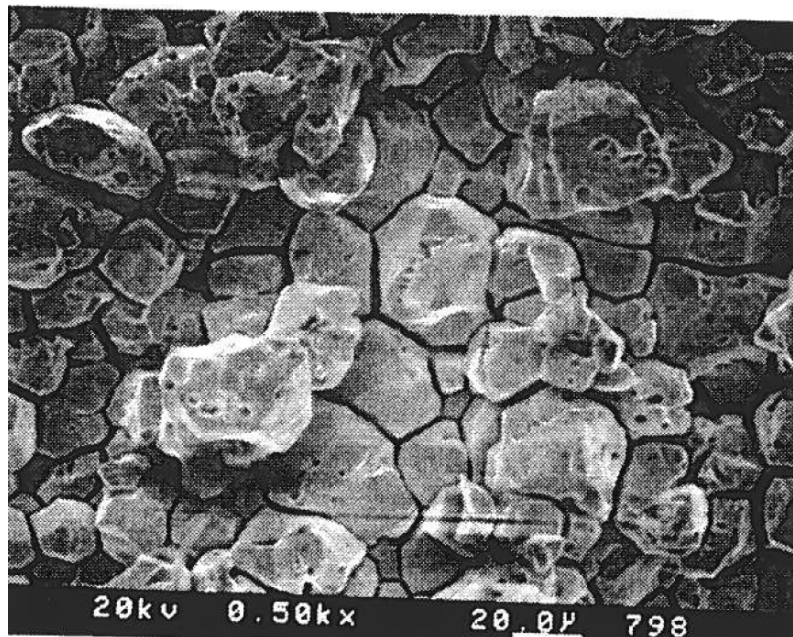


Figure 3-9. SEM image of surface of specimen after vapor phase exposure, showing IGA (500X magnification) [56].



Figure 3-10. SEM image of cross-sectioned specimen showing IGA depth of attack in the liquid exposed metal. The dashed line indicates the level of the original surface and the arrow points to the deepest IGA penetration (250x magnification) [56].

Table 3-10. Corrosion Rates for 304L Stainless Steel in Acidic Uranyl Nitrate Solutions [56].

Solution	Vapor Phase Corrosion Rate (mpy)	Liquid Phase Corrosion Rate (mpy)
A	120	110
B	100	110
C	110	140
D	80	110

3.3.3 WFE Tests at Oak Ridge National Laboratory Supporting Disposition of Melton Valley Waste

In the 1990s, Oak Ridge National Laboratory (ORNL) needed to process and dispose of transuranic (TRU) waste, which consisted of thick calcium carbonate, aluminum hydroxide, and magnesium hydroxide sludges suspended in solutions that were approximately 4 M sodium nitrate. Pilot-scale tests to concentrate this low-level liquid waste (LLW) were performed to demonstrate the effectiveness of a WFE unit [10], [57]. The system parameters studied were rotor speed, process fluid feed temperature and feed rate, and evaporator temperature.

The evaporator facility consisted of a 500-gallon mixing tank; an insulated 500-gallon preheat/feed tank; the WFE, which had a 5.4 ft² heat transfer surface area (see Figure 3-11); a product collection station; a heat exchanger to condense the distillate; a 250 gallon distillate receiver tank; cooling

water dichlorination unit; assorted piping and fluid transport media. The heating jacket of the evaporator was heated with 150 psig steam to 180 °C steam. The mixing tank could be heated with 50 psig steam to 147 °C. In addition to evaluating process variables, the equipment was inspected for corrosion problems and the effects of the waste on the evaporator heat transfer surface due to erosion-corrosion and scaling [10].

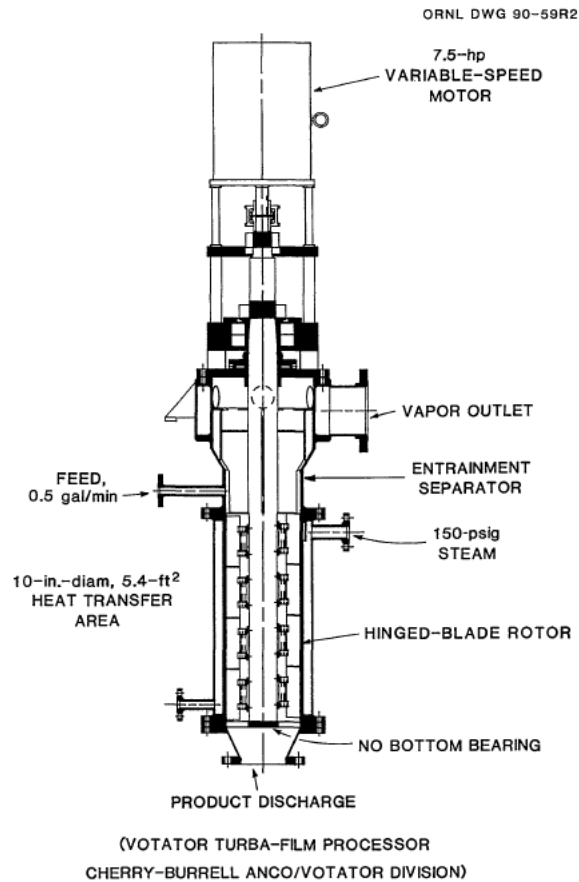


Figure 3-11. WFE for Pilot-Scale Tests at ORNL [10].

The composition of the waste simulant supernate and sludge that were tested are shown in Table 3-11 and Table 3-12, respectively. The liquid has a high silica concentration. Silica is known to cause scaling of heat transfer surfaces at high pH levels (> 9), particularly in the presence of magnesium. The reference cited reviewed the results from tests performed with supernate only. Another set of tests was to be performed with the sludge simulant as well. These tests were to evaluate the potential for erosion-corrosion. This reference has not been located yet.

Table 3-11. Liquid Waste Simulants for Pilot-Scale WFE Testing at ORNL [10].

Component	Concentration (g/L)
NaNO ₃	369.80
KNO ₃	28.30
Na ₂ CO ₃	15.90
NaCl	4.27
Ca(NO ₃) · 4H ₂ O	0.05
MgCl ₂ · 6H ₂ O	0.01
Na ₂ SiO ₃ · 9H ₂ O	2.48
NaOH	0.66

Table 3-12. Sludge Solids for Simulants for Pilot-Scale WFE Testing at ORNL [10].

Component	Concentration (wt % suspended solids)
Al(OH) ₃	6.5
CaCO ₃	74.6
Mg(OH) ₂	18.9

The tests consisted of a series of 40-gallon batch runs. For each batch, various process parameters were adjusted to investigate their impact on the process product. Table 3-13 shows the process parameters that were varied and the ranges that they were varied over. A total of 25 runs were performed with the supernate simulant. This combined with studies with water only added up to over 100 hours of WFE operating service.

Table 3-13. Process Parameter Values for WFE Testing at ORNL [10].

Process Parameters	Range
Rotor Speed (rpm)	250, 500, and 750
Pre-heat Tank Temperature (°F)	Ambient and 125
Evaporator Temperature (°F)	300 and 350
Process Fluid Feed Rate (gal/min)	0.1, 0.25, 0.5, 0.75, 1.0 and 1.2

The WFE was thoroughly inspected after the supernate studies. The rotor and stator that had been in service were severely eroded. Deep grooves were observed in the 316 stainless steel rotor. The soft rubber inside portion of the stator, which was fabricated from ethylene propylene diene monomer (EPDM), had deep gouges throughout. A significant amount of rust-type corrosion products was observed on the heat transfer surface of the WFE. The surface was also scarred, indicating abrasive wear or erosion had occurred. This was anticipated because during several of the experiments, the rotor could be heard rubbing against the sides of the evaporator. Some of the WFE blades also had rust-like corrosion products, and several of the blades appeared to be eroded. A close examination of one of the blades revealed that the bottom bushing holding the blade against a pin had slipped out of place. This allowed the bottom of the blade to rub against the side of the shell. Approximately 1/16 inch of the bottom of the blade had eroded. All the pins and bushings were damaged. The pins were bent outward from the shaft in the direction of the heat transfer shell. The pins were made from 304 stainless steel (although the design had originally called for Stellite) and were not strong enough to withstand the forces generated during operation. Due to this failure, it was recommended that the MOC for the pins be cold-work-hardened material or a strong, corrosion resistant metal like Ultimet (a nickel-based alloy). The heat transfer shell was inspected for leaks (i.e., dye penetrant) and wall loss. No loss of integrity or wall loss was detected.

In general, the equipment was durable, however areas associated with the rotating shaft were susceptible to overload if the materials were not strong enough.

3.3.4 Low Temperature, Vacuum WFE Developed by Columbia Energy

Columbia Energy and Environmental Services (CEES) designed and demonstrated a vacuum WFE [58], [59], [60]. The initial plans were to use the WFE to evaporate liquid radioactive waste in the Hanford tank farm. The WFE was designed to be modular and transportable, allowing it to be potentially located at any double shell tank (DST). Its principal purposes were to serve as a back-up to the primary vacuum evaporator and to accelerated concentration of DST and single shell tank (SST) wastes. In addition, a WFE was to be considered for the Effluent Treatment Facility as a means for minimizing secondary wastes. Pilot-scale and full-scale demonstrations were performed. The environmental conditions for each of the demonstrations were reviewed. However, the references that were reviewed contained little information regarding the MOCs. Additionally, the tests were short duration, and therefore it was difficult to evaluate long term material performance.

The WFE system that was tested is shown in Figure 3-12. This WFE augments traditional water removal through the usage of a high vacuum. The vacuum reduces the boiling point of water to approximately 50 to 60 °C. The system included a Rototherm evaporator assembly with a condenser with a 1 ft² heated surface (see Figure 3-13); a diesel generator; a water chiller; a vacuum system; cavity pumps; a feed preheater; and various piping, valves and instruments. The MOC for

the heat transfer surface was 316 stainless steel. However, the piping and valves for the feed bottoms and condensate were constructed of carbon steel.

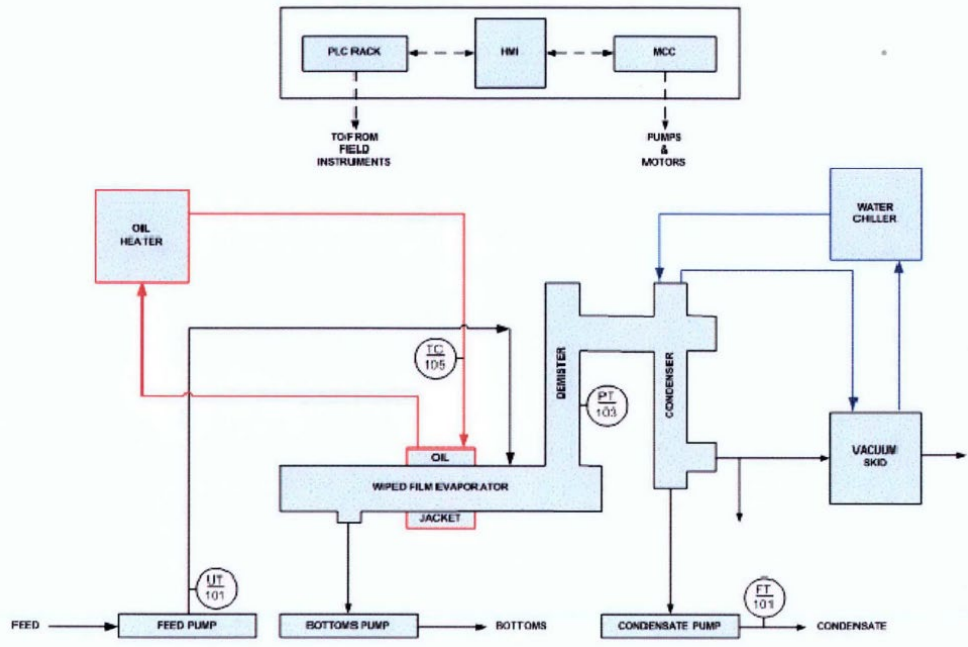


Figure 3-12. CEES Pilot Scale WFE System [59].



Figure 3-13. Pilot Scale Rotatherm WFE [59].

Two DST waste simulants (AN-105 and AN-107) [61] and one SST simulant (Dissolved Saltcake) [62] were tested in the pilot plant. The simulant compositions are shown in Table 3-14. Pilot scale testing was performed to accomplish the following objectives: assess the performance of the system (i.e., process parameters); assess system wear at regular intervals; and collect samples to

characterize the properties of the feed, bottoms and condensate. A sequence of batches that involved all 3 simulants was performed. The batch size was typically between 10-30 gallons.

Table 3-14. Waste Simulant Compositions for WFE Pilot Scale Tests [61], [62].

Component	AN-105 (M)	AN-107 (M)	SST Dissolved Salt Cake Simulant (M)
Hydroxide	3.42	0.02	0.485
Nitrite	2.41	1.33	0.424
Nitrate	2.66	3.71	2.51
Chloride	0.256	0.0516	0.0438
Fluoride	0.01	0.007	0.0316
Sulfate	0.008	0.086	0.09
TIC	0.209	1.4	0.475
TOC	0.299	3.36	0.287

The rapidly agitated, thin film processing configuration concentrated each simulant without fouling or equipment failure. It was recommended that studies with longer test duration be performed to provide additional longevity data, but the initial results were promising. Seal water to the evaporator rotor was temporarily lost during the test due to a kink in the supply line, and an off-normal noise was heard. Once the seal water was restored, the noise disappeared, and the unit functioned normally. No evidence of degradation of the rotor was noted. The carbon steel pipes associated with the WFE were rusted. The degree of corrosion observed was not mentioned. However, as a precaution it was recommended that these MOCs be upgraded to stainless steel. In addition to visual inspection of the condensate, the WFE performance was monitored by measuring the solution conductivity. The presence of rust in the system may have influenced these measurements.

The performance of the WFE MOCs during the pilot-scale tests was promising, although the testing time was limited. The shorter time may mean that failures due to the rotating shaft would not be observed. The lower temperature of the heat transfer surface may have served to reduce the degradation observed on less expensive stainless-steel materials.

A second set of pilot-scale WFE tests were conducted by Columbia Energy in 2010 [58]. The same three simulants were tested. Although it is not clearly stated, the size of the evaporator (1

ft²) and the manufacturer name (Rotatherm) suggest that it was the same evaporator that was tested in 2007. The feed rate for the tests ranged between 0.17 and 0.48 gallons/minute. The heating medium for the evaporator was oil at a temperature of approximately 360 °F (~182°C). Again, 10 to 30-gallon batches of simulant were processed through the WFE for these pilot scale tests. The total run time was approximately 33 hours.

The reference to the 2010 tests did not address any issues related to the performance of the materials [58]. No mention of the WFE MOCs was made in the paper either, however, given the description, size and manufacturer it is likely that it was the same one that was tested in 2007. Given the short time frame of the tests, limited degradation of 316L material would be observed given the environmental conditions above.

A full-scale demonstration of the modular WFE was performed in 2011 [59]. A photograph of the WFE is shown in Figure 3-14. The AN-105 simulant was utilized for the demonstration. The heat transfer surface area of the evaporator was 50 ft². The heating medium was 28 psig steam (~260 °F), and the vacuum system was operated such that the exit temperature was approximately 120 °F. The flow rate was varied between 8 and 10 gpm. The tests were conducted over a five-day period. A post-test inspection did not reveal significant degradation of any of the WFE components. However, longer-term testing would be necessary to demonstrate that the MOCs are adequate.

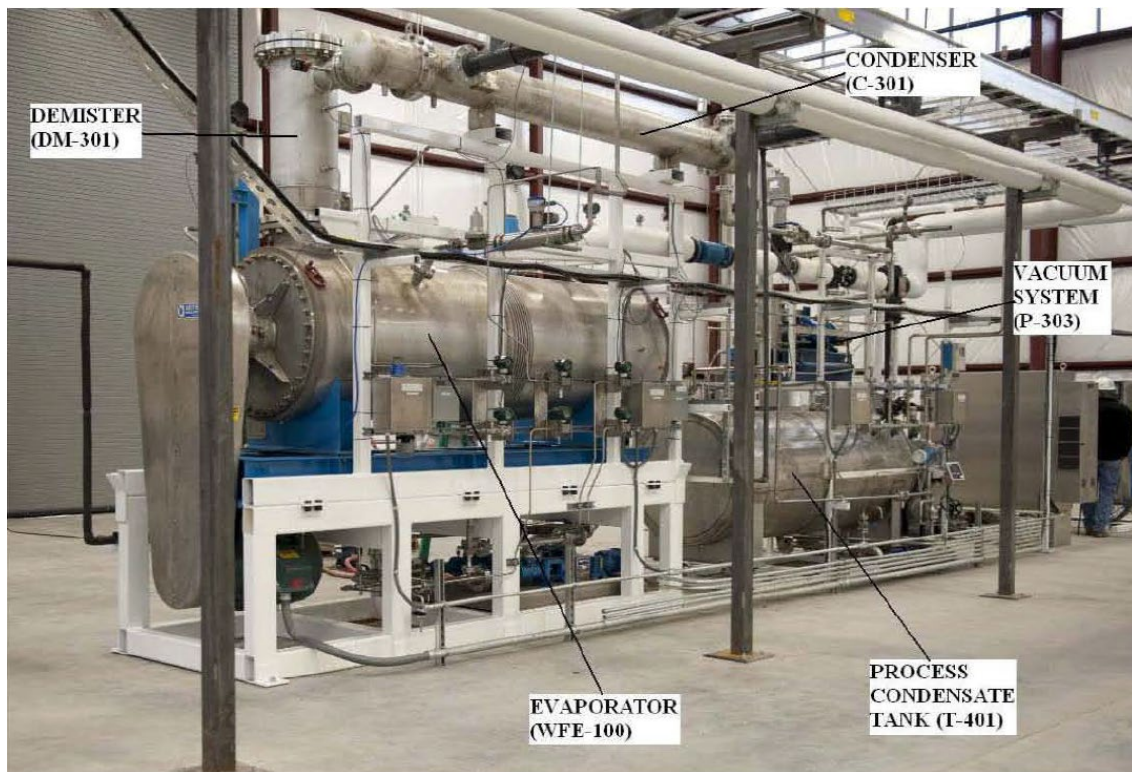


Figure 3-14. Full-Scale Rotatherm WFE [60].

3.3.5 Thin Film Dryer for Hanford Effluent Treatment Facility

A thin film dryer (TFD), also known as a WFE, manufactured by BUSS-SMS of Germany and distributed in the U.S. by the LCI corporation, is used as part of waste processing operations at the Effluent Treatment Facility (ETF) in the 200E Area of the Hanford Site [63]. It has been operational since 1995. The TFD is shown in Figure 3-15. The TFD is composed of a rotor and six flights of blades made from 316L housed inside a 365°F (185°C) steam heated drum (see schematic of LCI TFD in Figure 3-16). The internal surface of the drum is lined with Inconel Alloy 625. The flights of blades spin within 0.5 mm of the wall of the drum at a fixed speed of 252 RPM, which is equivalent to a blade tip speed of 26 ft/sec. During normal operation, feedwater (an aqueous brine) is injected into the top of the dryer. The water portion of the brine evaporates as it runs down the walls leaving solid material (dried salts) which is removed by the rotating blades. Two feedwater chemistries were used in the TFD. Table 3-15 shows the groundwater chemistry used during approximately 70% of operation. Table 3-16 shows the process condensate chemistry used during the balance of operation. As can be seen from the chemistry of the solutions, the pH ranges from 5 to 10.5 [64].



Figure 3-15. Hanford ETF Thin Film Dryer.

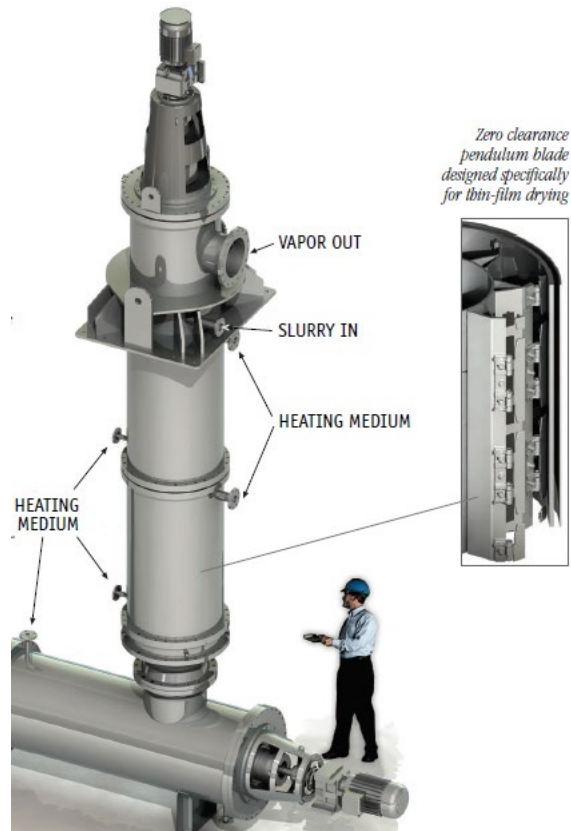


Figure 3-16 Schematic of an LCI TFD taken from Product Literature 2021.

Table 3-15 Groundwater Chemistry for TFD (70% operation) [64].

Component	Concentration (ppm)
Calcium	400
Potassium	1,680
Magnesium Hydroxide	11,960
Sodium	82,200
Chloride	4,050
Nitrate	54,100
Sulfate	118,000
Total Solids: 25 wt %	
Specific Gravity: 1.20	
pH: 10.5	
Alpha: 100 pCi/L	
Beta: 300 pi/L	

Table 3-16 Process Condensate Chemistry for TFD (30% Operation) [64].

Component	Concentration (ppm)
Ammonium	55,800
Calcium	160
Potassium	135
Magnesium	30
Sodium	27,100
Chloride	200
Nitrate	1,440
Sulfate	187,500
Total Solids: 25 wt %	
Specific Gravity: 1.16	
pH: 5.5	
Alpha: 3,800 pCi/L	
Beta: 1,500,000 pCi/L	

The TFD vessel has been replaced once and the rotor blades have been replaced several times. There were three instances between 1995-2001 where broken rotor blades were noted during an inspection and then replaced [65]. The vessel has also been replaced after getting scratched and gouged by a broken rotor. This became a much bigger problem when the scope of the waste waters treated at ETF was expanded to include groundwater and leachates. The groundwater formed a much harder solid on the inner wall of the vessel and the rotor blade failure rate increased significantly. Groundwater is no longer processed, but leachates are still processed. The Hanford 242-A evaporator process condensate, which ETF was designed to treat, creates a powder that is much easier on the rotor blades.

In 2001, a failure analysis was performed on several of the blades that had failed [64]. The new rotor and blades had been placed in service in May 2000 [65]. Within 3 months, by late Fall, the performance of the TFD had become inefficient. The poor performance was characterized by: 1) alarmingly loud noises (e.g., thumps, bangs, vibrations), 2) low feed rate capability (i.e., max of 0.4 gpm), 3) flushing frequency had increased from weekly to daily, and 4) occasional dryer plugging. In May 2001, the TFD was shut-down and inspected. Of the 36 blades, approximately 70% of the blades had failed.

The failure analysis was based on visual and photographic inspections of several of the failed blades in conjunction with background information on the operation of the TFD. Nine samples of the failed blades were sectioned from the TFD and viewed macroscopically and microscopically. Figure 3-17 shows a macroscopic view of a failed blade section. Figure 3-18 and Figure 3-19 show micrographs of the fracture surface that illustrate the failure mechanisms.



Figure 3-17 Macroscopic view of failed blade tip [64].

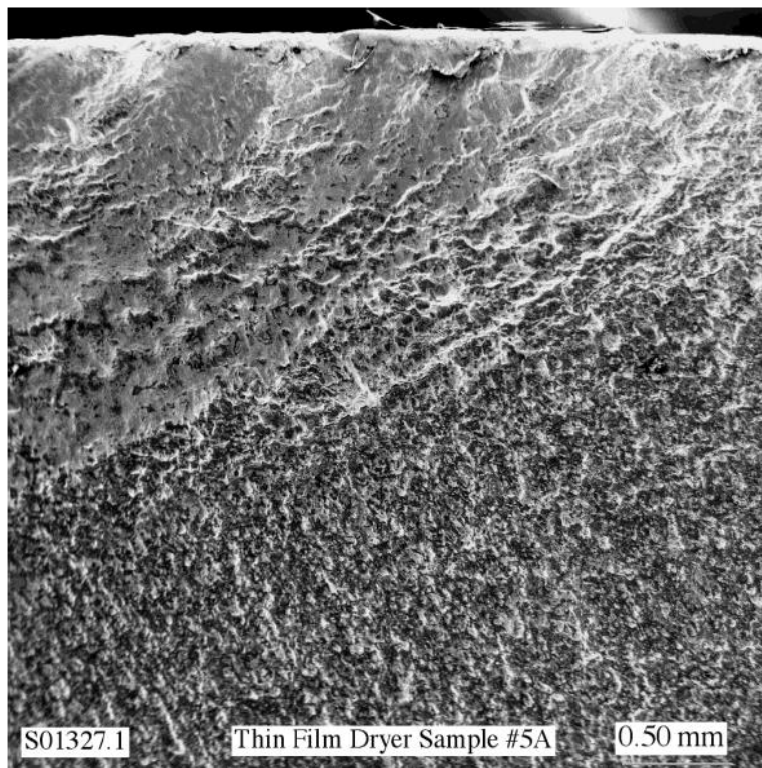


Figure 3-18. Failure by Chloride SCC or Corrosion Fatigue (see upper left) [64].

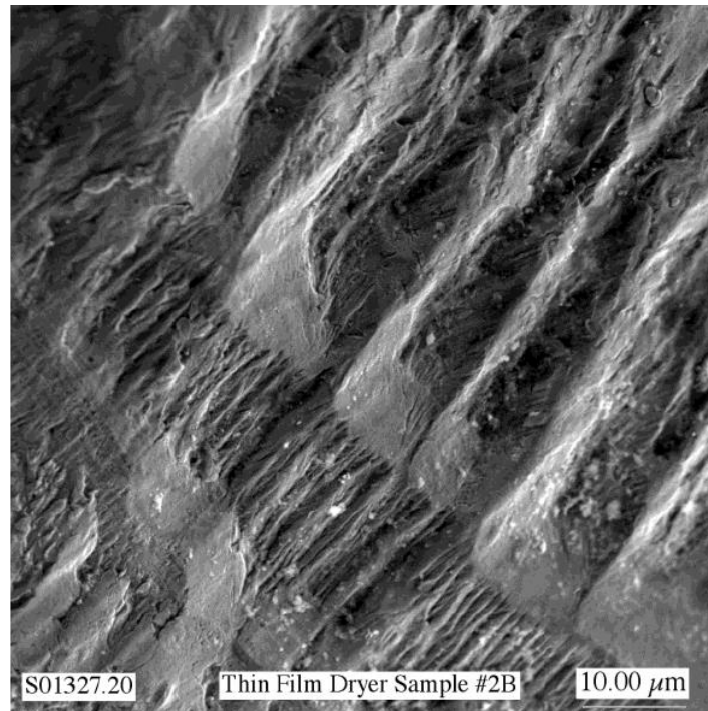


Figure 3-19 Failure by Fatigue [64].

Based on the visual inspection of the samples, the SEM work and a review of the operating conditions of the TFD, blade failures likely occurred due to chloride stress corrosion cracking, corrosion fatigue, cyclic fatigue, or some combination of these mechanisms. Some evidence of all three failure modes was discovered during the failure analysis process. More evidence was found to support chloride stress corrosion cracking and/or corrosion fatigue than was found for cyclic fatigue. No evidence of intergranular stress corrosion cracking was discovered during the analysis. This mode of failure was therefore eliminated as a possibility. No mention of erosion-corrosion of the blades was indicated in the report, despite the presence of solids although, it should be recognized that glass frit was not present in the waste.

In most cases, beach-marking indicated that cracks initiated at a stress riser formed where the hinge is welded to the blade and progressed radially outward toward the edge of the blade (see Figure 3-17). Two other contributing factors to failures were noted [66]. An increased build-up of hard scale, particularly with the ground water, was observed on the wall and the blade hinge area (see Figure 3-20). This build-up caused increased stresses on the blades as they tried to break the material into powder. Binding of the blade hinge due to accumulation of particles did not allow the hinge to remain in close contact with the wall. The result was inefficient evaporator operation and additional stresses on the other blades.

One other notable feature of this WFE is that it has a ‘hopper knocker’, which helps keep solids flowing through the dryer. The knocker is mounted to the exterior of the dryer using a bracket,

which eventually failed and breached the process wall. While the cause of this failure is unknown, the location of the failure suggests that fatigue may have been an issue.



Figure 3-20. Failed TFD rotor hinge.

3.3.6 Agitator Blade Performance in DWPF Sludge/Frit Slurries

Evidence of erosion caused by slurries that contained glass frit surfaced in early 1981 at an SRS pilot-plant testing facility [11]. Sludge/frit slurries were used in the melter slurry feed system. Examination of the centrifugal pump used in the feed system revealed substantial erosion wear on components. An erosion test apparatus (ETA) was constructed to investigate the performance of agitator blades in the sludge/frit slurries. Tests were performed in 50 mesh frit/sludge slurry and 200 mesh frit/water slurry. Figure 3-21 shows the relationship between the erosion-corrosion rates and the tip velocity for 304L stainless steel. The results show that erosion-corrosion rates at high velocities for the coarser 50 mesh frit were greater than that for the finer mesh frit. For example, at 10 ft/s, an erosion-corrosion rate of 20 mils/yr is predicted for 200 mesh (74 microns) frit service and 60 mils/yr is predicted for 50 mesh (297 microns) frit service. Care should be used in applying these results to the WFE. The test conditions were not well documented. If this test was for the SME/SRAT, they would have been performed under acidic conditions versus the alkaline conditions of the WFE. Solids concentration was also not reported. These values would represent bounding conditions because the test environment was at lower pH, higher temperature, and higher frit concentration than would be observed in the RD flowsheet.

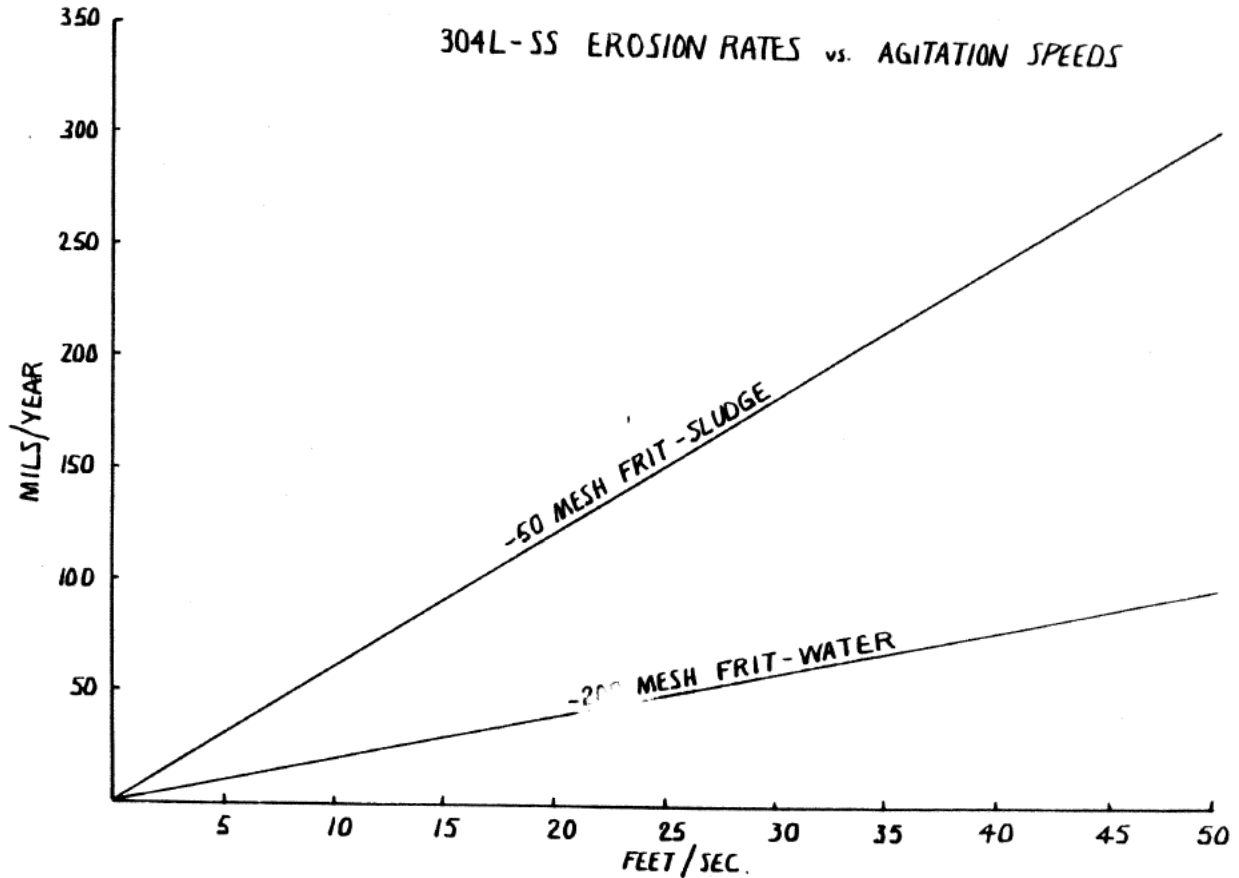


Figure 3-21. Erosion Test Apparatus Results [11]

Erosion-corrosion on the 1/3 scale SME/SRAT located at TNX was also evaluated [11]. Three batches of sludge/frit slurry were tested. Frit sizes in the batches were -200 mesh, -100 mesh, and -80 mesh for the 1st, 2nd, and 3rd batches, respectively. The agitator tip speed was 7 to 10 ft/sec. During formic acid addition, the pH ranged from 3 to 11. Temperatures also ranged from 30 °C to 102 °C. Maximum blade wear was anticipated near the blade edges and tips. Based on the ETA results and the wear measurements from these tests, a model was developed to predict the erosion-corrosion wear rate. Predicted erosion-corrosion rates for flat agitator blades, fabricated from 304L stainless steel, were on the order of 300 mils/year. Erosion-corrosion of pitched blades was approximately 75 mils/yr. Care should be used in applying these rates to the RD WFE as the pH and the temperature may not align with those conditions and, while the equipment was 1/3 the size of the prototypic equipment, the slurry particles were full scale, so scale must be considered to fully understand the results.

In later tests, a full scale dual use Hastelloy C-276 (C276) processing vessel, prototypic of DWPF SME/SRAT vessels was used for erosion-corrosion testing [12]. The agitator tip speed was 10 feet/sec. Although not defined, it is assumed that the environmental conditions would have been similar to those for the 1/3 scale tests. Severe erosion of the C276 agitator blades was observed.

To mitigate erosion-corrosion, significant design changes were made to the flat blades, which included the introduction of fully welded C276 blades. This agitator design was placed into service before non-radioactive simulant tests (cold runs) were performed in DWPF.

After the 18-month cold runs, the agitator blades were inspected for evidence of erosion-corrosion [12]. Degradation of the agitator blades was observed for the SME, where the glass frit is added. Prior to beginning radioactive operations, the blades were hard-faced with Stellite. Erosion-corrosion problems still plagued the agitator blades during operation. Additionally, coil failures began to occur due to the vortices created by the rectangular solid bar supports. A test program was conducted to evaluate more erosion-corrosion resistant alloys. The tests were conducted in a slurry pot in two different slurry-frit environments. The first slurry contained frit and water, while the second slurry contained the SME chemistry with simulated sludge, formic acid and frit. Test results indicated that there was a significant erosion-corrosion effect. Of the alloys tested, Ultimet, a nickel-based alloy, performed the best. Blade assemblies constructed from Ultimet were installed and have performed satisfactorily for more than 20 years. The conditions of these tests were significantly different than those that the WFE blades will be exposed to during the RD process (much lower pH). Therefore, these results would be conservative.

3.4 Bent Tube Evaporator Degradation and Failures

SRS has managed waste volume in the CSTF for more than 60 years by operating bent tube evaporators (BTE). These evaporators are operated at atmospheric pressure and require recycle to finish concentrating the waste [13]. The MOCs for the evaporators have been 304L stainless steel and Hastelloy G3 and G30, which are nickel-based alloys. In general, these materials have had a service life on the order of 10-20 years. The most vulnerable component of the evaporator system are the bent tubes. The bent tubes carry steam and operate at temperatures up to 180 °C and process liquid temperatures between 115 to 135 °C with hydroxide concentrations between 15 to 35 wt.% (i.e., pH is much greater than 14). The BTE is subject to fouling, corrosion and fatigue [13]. Testing and evaluations have been performed to assess the susceptibility of these materials to failure during service. One in-service failure of an evaporator occurred due to erosion. This case was reviewed for this evaluation.

3.4.1 *Corrosion Testing for Evaporator Materials*

The stainless steel and nickel-based alloys have also been tested in high temperature simulated wastes. The heat transfer surface for these tests simulated the operation of the evaporator steam tube bundle by use of a hot-wall test. The investigation performed electrochemical, immersion and hot-wall corrosion tests on 304L stainless steel, Hastelloy G3 and C276 materials in simulated acidic and alkaline solutions [16].

Table 3-17 shows the composition of the test solutions. The temperature at the hot wall was approximately 220 °C and the liquid was approximately 118 °C. The tests were conducted for 28 days. For the 304L stainless steel, a thick adherent deposit formed on the surface of the coupon. The general corrosion rate was 1.1 mpy. No localized corrosion was observed. For G3 alloy, the deposit was also observed, and the general corrosion rate was on the order of 0.1 mpy [16]. No general or localized corrosion was observed. Stress corrosion cracking tests with 304L stainless steel and G3 were performed in the 45 wt.% sodium hydroxide simulant at the boiling point. No significant indications of SCC were observed [67].

A hot-wall test was recently performed in the same simulants on the G3, G30 and Inconel 625 (625) nickel based alloys [17]. All alloys showed evidence of a small degree of localized corrosion. The degree of attack was acceptable for the G3 and G30 materials, but the 625 material showed less resistance to attack. Electrochemical and immersion tests were also performed on these materials at temperatures near the boiling point. Alloys G3 and G30 indicated no susceptibility to general or localized corrosion, while the 625 showed less resistance to localized mechanisms, particularly IGA. Based on material availability and performance, G30 was recommended.

Table 3-17. Composition of Simulated Alkaline Evaporator Solution [16].

Chemical Compound*	Dilute OH	Moderate OH	High OH
Hydroxide	3.8	14.5	45
Nitrate	17.3	12.8	N/A
Nitrite	3.1	11	N/A
Aluminate	2.2	7.6	N/A
Carbonate	0.5	1.6	N/A
Sulfate	0.6	0.4	N/A
Fluoride	0.03	0.01	N/A
Chloride	0.04	0.17	N/A
Silicate	0.05	0.05	N/A
Phosphate	0.04	0.1	N/A
Oxalate	0.05	0.04	N/A
Mercuric Nitrate	0.02	0.02	0.02

*Chemical compounds are sodium salts except for mercuric nitrate (Hg(NO₃)₂).

Similar corrosion tests were conducted on C276 in simulated wastes with a lower pH. The waste compositions are shown in Table 3-18. The four test solution represent a wide range of pH and chloride concentration. For the RD process, the results of tests performed in the pH 9 simulant (Solution D) are pertinent. It should be noted however, that the chloride levels for this simulant are higher than the typical amount observed in liquid waste in the CSTF, which is on the order of 1-5 ppm. Electrochemical and coupon immersion tests were performed at the boiling point temperature. Both tests indicated that C276 would have a low general corrosion rate and was essentially immune to localized corrosion in this environment. Hot-wall tests were performed in Solution C, a simulant with a lower pH. A thick, adherent deposit formed on the surface of the

sample. However, the general corrosion rate was very low, and no localized corrosion was observed. Therefore, the C276 material would be expected to be effective at pH values up to 9.

Table 3-18. Composition of Simulated Acidic Evaporator Solution [16].

Species	Concentration, ppm			
	Solution A	Solution B	Solution C	Solution D
Fluoride	7	28	133	<56
Formate	4	1	1	48804
Chloride	1669	1851	1014	1612
Nitrite	95	335	10	<1
Nitrate	36468	21294	46475	27614
Sulfate	33	203	167	736
Oxalate	16	18	13	103
Phosphate	1	-	1	<1
Insoluble solids	~15 wt%	~15 wt%	~15 wt%	~15 wt%
pH	2	6	4	~ 9

Failure of the 304L BTE tube bundle due to pitting corrosion has been observed [18]. Investigations revealed that these failures occurred during outages when the tube bundle was submerged in uninhibited well water. The temperatures in this case were primarily at the ambient conditions. The well water seeped beneath adherent deposits on the tube bundle and leached aggressive species from the deposits (e.g., halides, chromium, etc.), which led to crevice corrosion of the tube bundle [19]. Two improvements were made to mitigate this mechanism. First, it was required that inhibited water (pH>12) be utilized when the tube bundle is submerged during outages [19]. Secondly, more corrosion resistant materials were utilized for the tube bundle. The tube bundles that are in use currently are fabricated from either G3 or G30, which are nickel-based alloys [18].

Finally, periodic evaporator cleaning operations were considered. Over time, aluminosilicate deposits build up on the tube bundle for the 242-2H (2H) evaporator [68]. Since the 2H evaporator currently handles the DWPF recycle stream, this could be an issue for the evaporator in the RD process, particularly if it is operated at high temperatures (i.e., greater than 100 °C). A 1.5 M nitric acid solution, which is at a temperature of approximately 90 °C, is currently utilized to clean the tube bundle. The tube bundle is constructed of G3 material, and the evaporator vessel is constructed of 304L stainless steel. The cleaning solution is neutralized just before sending it to the evaporator receipt tank. The process typically lasts for a few days. The cleaning process was evaluated, and the risk of corrosion to either the vessel or the tube bundle was deemed to be low

[68]. Cleaning has been performed several times since 2000 with no evidence of significant attack on either the vessel or the tube bundle.

3.4.2 Failure Analysis of the 242-25H Evaporator Shell

The 242-25H (3H) evaporator was designed in the early 1990's, placed in-service in January 2000, was discovered to be leaking approximately 0.1 gallon/min in February of 2016 [23]. Figure 3-22 shows the salt that formed on the outside of the evaporator sheath due to the leak. The evaporator shell was constructed of Hastelloy G3, a nickel based alloy. After removal of the sheath and insulation surrounding the evaporator, the steam lance on the interior of the evaporator was activated. Three leak sites were visually identified on the bottom spherical head (see Figure 3-23). Ultrasonic (UT) thickness measurements of the bottom head were performed and indicated that the average metal loss was 0.2 inches over an area of approximately 190 in². This translates to a total eroded volume of 36 in³ or a total mass loss of 11 pounds after 16 years of service.

The pattern of degradation indicated by the UT exam, the proximity of the steam lance to the bottom spherical head, and the presence of undissolved solids suggested that slurry abrasive wear was the failure mechanism. Additionally, the angle of incidence between the steam lance spray and the bottom spherical head (approximately 45 °) was near the optimal value (approximately 30 °) for ductile materials such as G3. An evaluation utilizing an erosion rate model was performed to assess the likelihood that this was the failure mechanism [23]. The erosion rate given the parameters and assumptions in the model was proportional to the abrasive velocity cubed. The calculated fluid power based on the abrasive velocity of the steam lance would have easily produced the amount of erosion observed on the bottom spherical head. The presence of hard solid particles (e.g., undissolved solids) are also necessary to erode the surface. The hardness of the particles must exceed that of the eroded material, which in this case was the Hastelloy G3 (a Brinnell Hardness of 140). The model estimated that the observed erosion would be consistent with a stream that consisted of 0.5 wt.% of the solids that exceeded this hardness, coupled with an abrasive velocity that was approximately 15% of the lance steam exit velocity. These conditions could easily exist at the bottom spherical head.



Figure 3-22. Leakage from 3H Evaporator Shell [23].



Figure 3-23. Leakage from the Bottom Spherical Head of the 3H Evaporator [23].

This failure demonstrated that undissolved solids at a sufficient velocity and at a low incident angle could produce erosion of a ductile material, such as a stainless steel or nickel based alloy. It is recommended that during the design of the WFE, these parameters be considered when evaluating the blade and heat transfer surface for the possibility of erosion. The model used for the 3H evaporator erosion situation is recommended as a starting place, but other models may be available.

4.0 Anticipated Chemistry and Temperature Process Variables for the Recycle Diversion Process

SRR has developed a flowsheet for the RD process that provides estimates of the chemical and thermal environments for the process equipment. The following chemical and process assumptions were applied for the corrosion and erosion-corrosion evaluation [6].

- Nitric-Glycolic Acid Flowsheet implemented
- New DWPF Antifoam Momentive™ Y-17112 implemented with no new degradation species observed in the SMECT and OGCT condensate streams (due to the high stability of the new antifoam and the expectation that lower antifoam addition rates are expected relative to the current antifoam)
- Only SMECT and OGCT contributions to the RCT considered for baseline case
- RCT volume: 9,000 gallons (including NaOH and NaNO₂ additions to heel)
- RCT volume with added permanganate: 9,100 gallons
- Hydroxide: 0.16 M (assuming 75 gallons of 19.1 M NaOH added to heel, current addition amount)
- Nitrite: 0.16 M (due to addition of 215 gallons of 6.6 M NaNO₂ to heel)
- Permanganate: 0.018 M (assuming no reaction with glycolate, due to addition of 100 gallons of 6.6 M NaNO₂ to 9,000 gallons of RCT)
- Total Na⁺: 0.34 M
- Assumed liquid density: 1.0 g/mL
- 0.12 wt. % Frit 803 (due to addition of 41 kg frit per 9100-gallon RCT batch; partial dissolution expected)
- Frit 803 Composition: SiO₂ – 78.0 wt. %, Na₂O – 8.0 wt. %, B₂O₃ – 8.0 wt. %, Li₂O – 6.0 wt. %
- pH: 9 to ≥13 (due to addition of 50 wt. % NaOH to tank heel)
- Permanganate Reaction Time before filtration: 4-48 hours
- Initial Glycolate: 125 mg/L
- Final Glycolate (following permanganate strike): 1 mg/L
- RCT Temperature: 30 °C
- Filtration Temperature: <50 °C
- Evaporator Temperature: 60-120 °C (based on vacuum or atmospheric operations, respectively)
- Evaporator Concentrate Na⁺: 5.6 to 7.0 M
- Evaporator Concentration Factor: 16.3 to 20.3

The SMECT and OGCT Stream Compositions provided in Table 4-1 were used as a compositional basis in the RCT OLI Modeling report [4]. Since the OGCT is the stream from the melter off-gas, it is generally a more concentrated stream than the SMECT. Based on the expected chemical

additions (NaOH, NaNO₂ and NaMnO₄ reagent solutions) and the concentration factor in the melter, the concentrations of the major species in the chemically-adjusted RCT stream and the Diverted Recycle Evaporator Pot are provided in Table 4-2. The RCT sodium concentration after chemical additions is expected to be near 0.34 M Na⁺ and the RCT stream could be concentrated to as high as 7.0 M Na⁺ in the evaporator. This corresponds to a concentration factor of 20.3. Based on this factor and the chemical addition amounts, the expected concentrations of the other major species in the evaporator pot are provided in Table 4-2. Nitrite, hydroxide, and nitrate are the dominant anionic species. The concentrations of other species in the evaporator can be assumed to increase by the same factor if the species remain soluble and do not volatilize.

Evaluations of the fates of the various species of interest were based on relevant information provided in the referenced reports and general chemical knowledge of the species involved. In some instances, OLI Thermodynamic Modeling was utilized to provide additional insight regarding the fates of these species based on the conditions experienced during recycle diversion. Species known to be volatile can partition into the condensate streams and entrainment of species into the condensate can occur during foam over events. During evaporation, precipitates can form in the pot which may not be recovered from the evaporator without chemical cleaning with acid.

Table 4-1. SMECT and OGCT Compositions (RCT Feed).

Component	SMECT	OGCT
	M	
Al	1.6E-04	3.1E-03
Ca	6.1E-05	3.7E-04
Cr	<6.2E-06	1.5E-04
Fe	1.2E-04	2.3E-03
Hg	5.0E-04	1.1E-03
Mg	1.4E-05	1.2E-04
Mn	7.0E-05	1.1E-03
Na	1.6E-03	1.5E-02
Ni	<2.1E-05	1.8E-04
Si	2.1E-03	4.9E-03
Sr	3.2E-05	2.7E-06
Th	<7.8E-06	3.3E-05
U	<4.1E-05	1.3E-04
Zn	<2.8E-05	3.9E-05
formate	1.3E-03	<2.6E-03
oxalate	<1.1E-04	<1.3E-03
nitrate	5.8E-02	4.5E-02
nitrite	<2.2E-04	<2.5E-03
pH	1.6	0 to 1

Table 4-2. Estimated RCT and Recycle Diversion Evaporator Pot Major Species Concentrations Assuming 20.3x Evaporator Concentration Factor, and No Manganese Precipitation

Component	RCT	Recycle Diversion Evaporator Concentrate*
	M	
Na	0.34	7.0
nitrite	0.16	3.2
hydroxide	0.10	2.0
nitrate	0.045	0.92
Mn	0.18	0.37
pH	13	>14

* all other species expected to be <0.1 M

5.0 Assessment of Gaps and Recommendations for Testing

5.1 Transfer Lines

The transfer lines that are currently available, which are fabricated of 304L stainless steel, will likely be the first option for the RD process. For typical liquid radioactive waste service, the previous analysis demonstrated that negligible corrosion or erosion-corrosion damage is anticipated [8]. The RD process stream will have three potential differences: 1) a potentially lower pH, 2) the presence of permanganate, and 3) the presence of glycolate. Previous testing has shown that the presence of glycolate did not significantly impact the corrosion behavior of stainless steel in liquid waste simulants [38]. The presence of glycolate and permanganate at the anticipated levels for RD, and at a minimum hydroxide concentration of 0.1 M did not promote accelerated general corrosion or localized corrosion. On the other hand, these tests were not performed in simulants at the minimum pH levels (i.e., 9) or with the mercuric ion concentration for the proposed RD process. Given the tenaciousness of the oxide film on the stainless steel, the low halide concentrations, and relatively mild temperature, a significant increase in corrosion susceptibility at the conditions of the RD process would seem unlikely. However, screening tests to confirm that accelerated general and localized corrosion do not occur at the lower bound pH and in the presence of mercury are recommended.

The RD process has a similar undissolved solids concentration compared with those that were considered previously. However, the lower pH and presence of the mercuric ion may make the material more susceptible to erosion-corrosion. A screening test (e.g., rotating cylindrical electrode) is recommended to confirm that the 304L stainless steel is not susceptible to erosion-corrosion.

5.2 Cross Flow Filters

The CFF that are currently available, which are fabricated of sintered 316L stainless steel, will likely be the first option for the RD process. The testing environment (i.e., pH, halides, temperature) that was used for the LAWPS testing bounds the anticipated environment for the RD process. No significant general or localized corrosion of the 316L sintered metal surface was observed. Thus, no significant corrosion of the CFF would be anticipated during normal service or during the cleaning process.

No tests were performed to assess the CFF for susceptibility to erosion-corrosion tests under the LAWPS conditions. As with the transfer lines, a screening test (e.g., rotating cylindrical electrode) is recommended to confirm that the sintered 316L stainless steel is not susceptible to erosion-corrosion. These tests should cover a range of pHs that considers the filter cleaning process as well as the pH of the RD process stream.

5.3 Wiped Film Evaporators

The failure analysis of the TFD for the ETF at Hanford indicated that the 316L stainless steel blades had failed by chloride stress corrosion cracking, corrosion fatigue or fatigue. Failures of WFE in pilot-plant studies and actual service have been external to the vessel where the blades and heat transfer system are located. The failure mechanisms have been fatigue or wear (erosion) due to the movement of the rotating shaft. The failures were either at bearings, mechanical seals, or constrained supports. Careful design of the shaft train (i.e., consideration of both thermal and mechanical stresses), material selection (e.g., avoid situations where tungsten-carbide contacts the waste), and plans for maintenance of these areas that avoid contamination and dose exposure are recommended. Due to the moving shaft failures, mechanisms such as erosion or fatigue may occur within a time frame of relevance to the facility operator. The risk, probability, and consequence of failure may be minimized by designing the WFE with these considerations in mind.

The temperature of the WFE for the RD process is anticipated to be either 60 °C or the atmospheric boiling point of the waste (≤ 120 °C). From a corrosion standpoint, if the temperature is 60 °C or less for the RD process chemistry, the corrosion data indicate that a 300 series stainless steel would likely be appropriate for the vessel and the heat transfer surface. On the other hand, for temperatures approaching 120 °C, a nickel-based alloy such as G30 or Ultimet, which is used for the BTE tube bundle, may be more suitable for long term service.

There have been no long-term erosion-corrosion studies for either the 300 series stainless steel or the nickel-based alloy conducted at the RD process conditions. However, failure of the 3H evaporator suggests that the at a sufficient velocity and at a low incident angle could produce erosion of a ductile material, such as a stainless steel or nickel based alloy. It is recommended that

during the design of the WFE, these parameters be considered when evaluating the blade and heat transfer surface for the possibility of erosion. The model used for the 3H evaporator erosion situation is recommended as a starting place, but other models may be available.

The pilot-scale and full-scale demonstration by CEES, which used 316L stainless steel, for the low temperature, vacuum evaporator were short term tests that did not fully test the durability of the WFE. The closest analog for these has been the ETA tests at the SRS pilot test facility and the Slurry Pot tests at SRNL [11]. As with the transfer lines and the CFF, a screening test (e.g., rotating cylindrical electrode) is recommended to confirm that the stainless steel and the nickel-based alloys are not susceptible to erosion-corrosion. The results of these tests could be used to determine conditions for longer term tests if needed (e.g., slurry pot).

6.0 Conclusions

The potential for erosion-corrosion for the transfer lines and key unit operations (cross flow filters and wiped film evaporator) was evaluated for the proposed recycle diversion process. The evaluation reviewed the literature on performance of stainless steel and nickel-based alloys at the proposed RD process chemistry, identified potential gaps in the data, and recommended testing. The conclusions and recommendations for the transfer lines and unit operations are presented below.

Transfer Lines

- The RD process chemistry conditions are similar to those that were evaluated previously. The previous evaluation concluded that no accelerated corrosion or erosion-corrosion of the 304L pipelines would be anticipated. Recent testing for the glycolic flowsheet and the glycolate destruction process indicated a low susceptibility to corrosion at the current conditions as well.
- However, the testing conditions were at pH 13, whereas a minimum pH of 9 is proposed for the RD process. Screening tests to confirm that accelerated general, localized corrosion, and erosion-corrosion do not occur at the lower bound pH are recommended.

Cross Flow Filters

- The RD process chemistry and the filter cleaning operation were reviewed. Data from corrosion testing performed for LAWPS indicates that the sintered 316L stainless steel materials have a low propensity for general or localized corrosion.
- No tests were performed to assess the CFF for susceptibility to erosion-corrosion under the Hanford LAWPS conditions. As with the transfer lines, a screening test (e.g., rotating cylindrical electrode) is recommended to confirm that the sintered 316L stainless steel is not susceptible to erosion-corrosion. These tests should cover a range of pHs that considers the filter cleaning process as well as the pH of the RD process stream.

Wiped Film Evaporators or Thin Film Dryers

- The performance of materials during pilot-scale and full-scale demonstrations, as well as field performance was reviewed.
- The failure analysis of the TFD for the ETF at Hanford indicated that the 316L stainless steel blades had failed by chloride stress corrosion cracking, corrosion fatigue or fatigue.
- Some of the failures of WFEs in pilot-plant studies and actual service have been external to the vessel where the blades and heat transfer system are located. The failure mechanisms have been fatigue or wear (erosion) of bearings and seals due to the movement and/or misalignment of the rotating shaft. These failures in some instances have resulted in erosion of the agitator blades and light scarring of the heat transfer surface. Careful design of the shaft train (i.e., consideration of both thermal and mechanical stresses), material selection (e.g., avoid situations where tungsten-carbide contacts the waste), and plans for maintenance of these areas that avoid contamination and dose exposure are recommended. Due to the moving shaft, failure mechanisms such as erosion or fatigue may happen. The risk, probability and consequence of failure may be minimized by designing the WFE with these considerations in mind.
- The temperature of the WFE for the RD process may be either 60 °C or the atmospheric boiling point of the waste (~120 °C). From a corrosion standpoint, if the temperature is 60 °C or less for the RD process chemistry, the corrosion data indicate that a 300 series stainless steel would likely be appropriate for the vessel and the heat transfer surface. On the other hand, for temperatures approaching 120 °C, a nickel-based alloy such as G30 or Ultimet, which is used for the BTE tube bundle, may be more suitable for long term service.
- There have been no long-term erosion-corrosion studies for either the 300 series stainless steel or the nickel-based alloy conducted at the RD process conditions. As with the transfer lines and the CFF, a screening test (e.g., rotating cylindrical electrode) is recommended to confirm that the stainless steel and the nickel-based alloys are not susceptible to erosion-corrosion. The results of these tests could be used to determine conditions for longer term tests if needed (e.g., slurry pot). Engineering models may also be used to assess the likelihood of erosion of the blade and heat transfer surface given the wt.% of undissolved solids and the slurry abrasive velocity generated by the movement of the WFE blades.

7.0 References

- [1] W. D. King, "Task Technical and Quality Assurance Plan for DWPF Recycle Diversion: Glycolate Hydrogen Generation and Mitigation, Recycle Chemistry, and Evaporator Corrosion and Erosion Evaluations; and Recycle Simulant Formulation," SRNL-RP-2021-00538, Revision 0, Savannah River National Laboratory, Aiken, SC, April 2021.
- [2] G. C. Winship, "Diversion of DWPF Recycle from HLW Tanks Farms: Systems Engineering Alternatives Analysis," G-AES-S-00005, Rev. 0, Savannah River Remediation, Aiken, SC, 2019.

- [3] "'Defense Waste Processing Facility Recycle Diversion Block Flow Diagram", M-M5-G-00683, Revision A, March 2021."
- [4] D. B. Henley, "Initial OLI Runs in Support of the DWPF Recycle Diversion Project," SRR-LWE-2021-00016, Rev. 0, Savannah River Remediation, Aiken, SC, March 2021.
- [5] K. J. Imrich, "LAWPS Mott Filter Electrochemical and Flow-Through Corrosion Tests," SRNL-STI-2016-00292, Revision 0, Savannah River National Laboratory, Aiken, SC, June 2016.
- [6] W. D. King, "Evaluations of the Fates of Actinides, Mercury, Iodine, and Alkaline Earth Metals During DWPF Recycle Diversion," To Be Issued, Savannah River National Laboratory, Aiken, SC, June 2021.
- [7] C. Baker, "Wiped Film Evaporator (WFE) Sizing-DWPF Recycle Diversion Project," Presentation, Savannah River Remediation, Aiken, SC, 2021.
- [8] B. J. Wiersma, "A Structural Integrity Evaluation of the Tank Farm Waste Transfer System," WSRC-TR-2005-00532, Revision 1, Savannah River National Laboratory, Aiken, SC, July 2014.
- [9] D. A. Jones, Principles and Prevention of Corrosion, New York, NY: Macmillan Publishing Co., 1992.
- [10] M. D. Boring, "Concentration of Melton Valley Storage Tank Surrogates with a Wiped Film Evaporator," ORNL/TM-12768, Oak Ridge National Laboratory, Oak Ridge, TN, August 1994.
- [11] P. L. Graf, "Erosion Wear by Frit Slurries," DPST-82-545, Savannah River Laboratory, Aiken, SC, 1982.
- [12] K. J. Imrich, "Overview of Corrosion, Erosion, and Synergistic Effects of Erosion and Corrosion in the WTP Pretreatment Facility," SRNL-STI-2015-000041, Rev. 0, Savannah River National Laboratory, Aiken, SC, March 2015.
- [13] C. B. Goodlett, "Concentration of Aqueous Radioactive Waste with Wiped Film Evaporators," DP-MS-75-17, Savannah River Laboratory, Aiken, SC, November 1975.
- [14] J. A. Donovan, "Metallographic Examination of Failed Stud from Wiped Film Evaporator," DPST-75-266, Savannah River Laboratory, Aiken, SC, March 1975.
- [15] P. R. Roberge, Erosion-Corrosion, Houston, TX: NACE International, 2004.
- [16] G. T. Chandler, "Hot-wall Testing of Simulated High Level Nuclear Waste," in *Corrosion '95*, Orlando, FL, 1995.
- [17] J. I. Mickalonis, "Corrosion Testing of Alternate Materials for the 242-25H Evaporator Replacement," SRNL-STI-2017-00562, Rev. 0, Savannah River National Laboratory, Aiken, SC, August 2017.
- [18] C. F. Jenkins, "HLW Evaporator Tube Bundle: Evaluation of Corrosion Failure Modes," SRT-MTS-2002-40070, Savannah River Technology Center, Aiken, SC, May 2002.
- [19] C. F. Jenkins, "Basis and Recommendations for Caustic Additions to Idled Waste Evaporators," SRT-MTS-935068, Savannah River Technology Center, Aiken, SC, May 1993.
- [20] "ASTM G40-10b, Standard Terminology Related to Wear and Erosion," West Conshocken, PA, ASTM International, 2010.
- [21] M. R. Duignan, "RPP-WTP Slurry Wear Evaluation: Literature Review," WSRC-TR-2001-00156, Rev. 0, Savannah River Technology Center, Aiken, SC, March 2001.
- [22] I. Finnie, "Erosion of Surface by Solid Particles," *WEAR*, vol. 3, pp. 87-103, 1960.
- [23] C. H. Keilers, "Failure Evaluation of Savannah River Site High-Level Waste Evaporator 252-25H," in *WM2018 Conference, Paper no. 18480*, Phoenix, AZ, March 18-22, 2018.
- [24] W. L. Daugherty, "Replacement High Level Waste Evaporator Tube - Flaw Evaluation," SRT-MTS-945104, Savannah River Technology Center, Aiken, SC, July 1994.

- [25] J. R. Divine, "Reports of Experimentation," Pacific Northwest Laboratory, Richland, WA, 1986.
- [26] B. J. Wiersma, "Coupon Immersion Testing in Simulated Hazardous Low Level Waste," WSRC-TR-91-493, Savannah River Technology Center, Aiken, SC, August 1991.
- [27] E. D. D. Doring, *Corrosion Atlas*, 2nd Edition, Amsterdam: Elsevier, 1991.
- [28] J. R. Davis, *Understanding the Basics of Corrosion*, Materials Park, OH: ASM International, 2000.
- [29] A. J. Sedriks, *Corrosion of Stainless Steels*, 2nd Edition, New York: John Wiley and Sons, 1996.
- [30] Z. Szklarska-Smialowska, *Pitting and Crevice Corrosion*, Houston, TX: NACE International, 2005.
- [31] R. S. Ondrejcin, "SRP Waste Compatibility with 304L Stainless Steel," DPST-78-303, Savannah River Laboratory, Aiken, SC, April 1978.
- [32] J. H. Phillips, *Corrosion*, vol. 15, p. 450t, 1959.
- [33] B. J. Wiersma, "Constant Extension Rate Tensile Tests on 304L Stainless Steel in Simulated Hazardous Low-Level Waste," WSRC-TR-92-229, Savannah River Technology Center, Aiken, SC, 1992.
- [34] A. J. Sedriks, *Stress Corrosion Cracking Test Methods*, Houston, TX: NACE International, 1990.
- [35] C. F. Jenkins, "H-Area CTS Loop, Cleanout Port No. 3 Replacement," 200-H Area Metallurgical Report, Savannah River Laboratory, Aiken, SC, 1983.
- [36] K. B. Martin, "CSTF Corrosion Control Program, Program Description Document," WSRC-TR-2002-00327, Rev. 9, Savannah River Remediation, Aiken, SC, 2015.
- [37] J. I. Mickalonis, "Corrosion Impact of Alternate Reductant on DWPF and Downstream Facilities," SRNL-STI-2014-00281, Rev. 0, Savannah River National Laboratory, Aiken, SC, November 2014.
- [38] J. Mickalonis, "Impact of Glycolate Anion on Aqueous Corrosion in DWPF and Downstream Facilities," SRNL-STI-2015-00482, Revision 3, Savannah River National Laboratory, Aiken, SC, January 2019.
- [39] C. Martino, "Thermolytic Hydrogen Generation Testing of Tank 22 Material," SRNL-STI-2018-00385, Rev. 0, Savannah River National Laboratory, Aiken, SC, 2018.
- [40] J. Zamecnik, "Permanganate Oxidation of Defense Waste Processing Facility (DWPF) Recycle Collection Tank (RCT) Simulants – Protocol Runs for Nominal and Chemical Process Cell (CPC) Foamover Conditions," SRNL-STI-2019-00292, Savannah River National Laboratory, Aiken, SC, 2019.
- [41] R. E. Fuentes, "Impact of Permanganate Oxidation of Glycolate on Corrosion of the Defense Waste Processing Facility (DWPF) Recycle Collection Tank (RCT), Transfer-line and Tank 22 Materials of Construction (MoC)," SRNL-STI-2019-00742, Savannah River National Laboratory, Aiken, SC, January 2019.
- [42] D. P. Lambert, "Sludge Batch 9 Simulant Runs Using the Nitric-Glycolic Acid Flowsheet," SRNL-STI-2016-00319, Rev. 0, Savannah River National Laboratory, Aiken, SC, November 2016.
- [43] C. A. Nash, "Permanganate Oxidation of Actual Defense Waste Processing Facility (DWPF) Slurry Mix Evaporator Condensate Tank (SMECT) and Offgas Condensate Tank (OGCT) Samples to Remediate Glycolate," SRNL-STI-2020-00012, Rev.0, Savannah River National Laboratory, Aiken, SC, March 2020.
- [44] W. S. Morrison, "DWPF Abrasion Tests Data Summary," Project 1780, Savannah River Laboratory, Aiken, SC, June 1985.
- [45] C. L. Trivelpiece, "Tank 40 Waste Acceptance Product Specifications (WAPS) Solids and Chemical Analysis (2018)," SRNL-STI-2018-00318, Savannah River National Laboratory, Aiken, SC, September 2018.
- [46] J. T. Gee, "DWPF Materials Evaluation Summary Report," WSRC-TR-96-0217, Westinghouse Savannah River Company, Aiken, SC, September 1996.

- [47] G. T. Chandler, "Impact of DWPF Frit Carryover to High Level Waste Tank Farm," SRT-MTS-95-2069, Savannah River Technology Center, Aiken, SC, December 1995.
- [48] "Database for DWPF transfers to the Tank Farm," Washington Savannah River Company, Aiken, SC.
- [49] P. E. Zapp, "Potential for Erosion Corrosion of Stainless Steel Components in the Late Wash Facility," SRT-MTS-94-2051, Savannah River Technology Center, Aiken, SC, December 1994.
- [50] B. K. Roberts, "Failed Evaporator Bottoms Line," 200-H Area Metallurgical Report, Savannah River Laboratory, Aiken, SC, August 1979.
- [51] "Piping Flexibility Analysis for Tanks 4, 5, 6, and 8 to FDB-2," Drawing W718173, Aiken, SC, August 1988.
- [52] J. I. Mickalonis, "LAWPS Mott Filter and Flow Through Corrosion Tests," SRNL-STI-2016-00242, Savannah River National Laboratory, Aiken, SC, May 2016.
- [53] "Pretreatment Engineering Platform Phase 1 Final Test Report," WTP-RPT-197, Rev. 0, Pacific Northwest National Laboratory, Richland, WA, December 2009.
- [54] L. L. Kilpatrick, "Wiped Film Evaporator Process for Producing Defense Waste Salt Cake," DPST-82-398, Savannah River Laboratory, Aiken, SC, April 1980.
- [55] J. I. Mickalonis, "Slurry Pump Compatibility Testing," WSRC-TR-2000-00004, Savannah River Technology Center, Aiken, SC, January 2000.
- [56] P. E. Zapp, "Corrosion of 304L Stainless Steel in Wiped-Film Evaporator Solutions," WSRC-RP-89-1336, Savannah River Laboratory, Aiken, SC, December 1989.
- [57] T. B. Caldwell, "Feasibility Study for Using a Package Evaporator System for the Defense Waste Processing Facility (DWPF) Recycle," LWO-CES-2008-00076, Rev. 0, Washington Savannah River Company, Aiken, SC, January 2009.
- [58] A. R. Tedeschi, "Application of a Thin Film Evaporator System for Management of Liquid High Level Wastes at Hanford," in *WM2010 Conference*, Phoenix, AZ, 2010.
- [59] A. R. Tedeschi, "Pilot Scale Test Results of a Thin Film Evaporator System for Management of Liquid High-Level Waste at the Hanford Site, Washington, USA," in *WM2011 Conference*, Phoenix, AZ, 2011.
- [60] A. R. Tedeschi, "Full Scale Testing Technology Maturation of a Thin Film Evaporator for High-Level Liquid Waste Management at Hanford," in *WM2012 Conference*, Phoenix, AZ, 2012.
- [61] R. E. Eibling, "Hanford Waste Simulants Created to Support the Research and Development on the River Protection Project - Waste Treatment Plant," WSRC-TR-2000-00338, Savannah River Technology Center, Aiken, SC, 2001.
- [62] S. D. Rassat, "Cold Dissolved Saltcake Waste Simulant Development, Preparation and Analysis," PNNL-14194, Rev. 1, Pacific Northwest National Laboratory, Richland, WA, May 2003.
- [63] S. Goetsch, "Effluent Treatment Facility - Challenged to Meet Environmental Restoration," in *International Low-Level Waste Conference*, Baltimore, MD, November 1992.
- [64] G. Edgemon, "Failure Analysis of Blade Failures on LCI Thin Film Dryer at the 200-Area Effluent Treatment Facility," 0101-FDH-018-008, HiLine Engineering, Richland, WA, August 2001.
- [65] D. E. Scully, "ETF Thin Film Dryer," Richland, WA, June 2001.
- [66] G. Millward, "Short Term Corrective Actions for Re-start of Thin Film Dryer," Richland, WA, August 2001.
- [67] G. T. Chandler, "Corrosion Performance of Alloy G3 and 304L Stainless Steel in Simulated High Level Waste Evaporator Solutions and Assessment of Service Life for Evaporator Tubes," in *Corrosion 96*, Denver, CO, 1996.

- [68] B. J. Wiersma, "An Assessment of Materials Performance During Chemical Cleaning of the 242-16H Evaporator," WSRC-TR-2006-00305, Savannah River Technology Center, Aiken, SC, October 2006.

Distribution:

cj.bannochie@srnl.doe.gov
alex.cozzi@srnl.doe.gov
mark.duignan@srnl.doe.gov
richard.edwards@srs.gov
Brenda.Garcia-Diaz@srnl.doe.gov
connie.herman@srnl.doe.gov
dennis.jackson@srnl.doe.gov
Brady.Lee@srnl.doe.gov
Joseph.Manna@srnl.doe.gov
daniel.mccabe@srnl.doe.gov
Gregg.Morgan@srnl.doe.gov
frank.pennebaker@srnl.doe.gov
michael.poirier@srnl.doe.gov
William.Ramsey@SRNL.DOE.gov
eric.skidmore@srnl.doe.gov
michael.stone@srnl.doe.gov
kenneth.wells@srs.gov
Boyd.Wiedenman@srnl.doe.gov
bill.clark@srs.gov
jeffrey.crenshaw@srs.gov
james.folk@srs.gov
Curtis.Gardner@srs.gov
Pauline.hang@srs.gov
Anna.Murphy@srs.gov
tony.polk@srs.gov
Anthony.Robinson@srs.gov
mark-a.smith@srs.gov
patricia.suggs@srs.gov
thomas.temple@srs.gov
william02king@srnl.doe.gov
michael.hay.srnl.doe.gov
stephanie.taylor@srnl.doe.gov
Stephen.harris@srnl.doe.gov
charles.nash@srnl.doe.gov
terri.fellinger@srs.gov
azikiwe.hooker@srs.gov
Patricia.Lee@srnl.doe.gov
seth.hunter@srnl.doe.gov
sean.noble@srnl.doe.gov
chris.martino@srnl.doe.gov
charles.crawford@srnl.doe.gov
arthur.wiggins@srs.gov
david.wallace@srs.gov
stephanie.harrington@srs.gov
rachel.seeley@srs.gov
christine.baker@srs.gov
ryan.mcnew@srs.gov
bill.holtzscheiter@srs.gov
david.henley@srs.gov
Records Administration (EDWS)